A Theoretical Study of the Mechanism of the Water-Catalyzed HCl Elimination Reactions of CHXCl(OH) (X = H, Cl) and HClCO in the Gas Phase and in Aqueous Solution

David Lee Phillips,*,† Cunyuan Zhao,*,‡ and Dongqi Wang†

Department of Chemistry, The University of Hong Kong, Pokfulam Road, Hong Kong, and School of Chemistry & Chemical Engineering, Sun Yat-Sen University, Guangzhou 510275, People's Republic of China

Received: June 6, 2005; In Final Form: August 20, 2005

A systematic ab initio investigation of the water-assisted decomposition of chloromethanol, dichloromethanol, and formyl chloride as a function of the number of water molecules (up to six) building up the solvation shell is presented. The decomposition reactions of the chlorinated methanols and formyl chloride are accelerated substantially as the reaction system involves additional explicit coordination of water molecules. Rate constants for the decomposition of chlorinated methanols and formyl chloride were found to be in reasonable agreement with previous experimental observations of aqueous phase decomposition reactions of dichloromethanol [$CHCl_2$-(OH)] and formyl chloride. For example, using the calculated activation free energies in conjunction with the stabilization free energies from the ab initio calculations, the rate constant was predicted to be $1.2-1.5 \times 10^4$ s^{-1} for the decomposition of formyl chloride in aqueous solution. This is in good agreement with the experimental rate constant of about 10^4 s^{-1} reported in the literature. The mechanism for the water catalysis of the decomposition reactions as well as probable implications for the decomposition of these chlorinated methanol compounds and formaldehydes in the natural environment and as intermediates in advanced oxidation processes are briefly discussed.

I. Introduction

Chlorinated methanols and formaldehydes are of interest in several areas of chemistry.[1−23] Chlorinated hydrocarbons are frequent pollutants of drinking water, and their degradation by a variety of methods and their reaction mechanisms are of intense interest.[7−19] In particular, advanced oxidation processes such as UV/hydrogen peroxide, UV/ozone, ozone/hydrogen peroxide, and electron beam radiation produce the highly reactive OH radical to induce decomposition of chlorinated hydrocarbons in drinking water supplies, and it is important to understand the mechanism of the oxidative decay cascade that can be observed by conductance changes.[7−18] To assign a kinetic component of a sequence of conductance changes to an elementary step in the ozone- or OH radical-caused oxidation cascade, it is important to determine the reaction kinetics independently.[10,19] This has been done experimentally for the kinetics of decomposition of phosgene (Cl_2CO)[10] and formyl chloride (HClCO).[19] Our present study examines the decomposition of selected chloromethanols and formyl chloride in the presence of water.

Chloromethanols have been experimentally observed in both low temperature matrices[4] and the gas phase[5,6] and, in both environments, decompose into formaldehydes and HCl in the dark. In the gas phase, the decomposition of $CH_2Cl(OH)$ into H_2CO + HCl was observed to have a rate constant of $(1.6 \pm 0.1) \times 10^{-3}$ s^{-1} in 30 cm diameter glass chamber.[5] The decay of $CH_2Cl(OH)$ was much faster in a smaller 20 cm stainless steel chamber, and it was suggested that measurements in both the glass and the stainless steel chambers may have a heterogeneous component, and the reported lifetime of 660 s for the homogeneous decay was considered to be a lower limit.[5] Subsequent studies for $CH_2Cl(OH)$, $CHCl_2(OH)$, and $CCl_3(OH)$ found that they decayed to their corresponding formaldehyde and HCl with rate constants of $(3.4 \pm 0.2) \times 10^{-3}$, $(5.5 \pm 0.3) \times 10^{-3}$, and $(9.9 \pm 0.2) \times 10^{-3}$ s^{-1}, respectively, in a gas phase chamber at Wuppertal.[6] The decay rates of these chloromethanols were observed to increase with increasing contact with the reactor walls indicating that there is some heterogeneous decay.[6] MP2/6-31G** calculations for the gas phase homogeneous decomposition of $CCl_3(OH)$ into Cl_2CO + HCl estimated a rate constant of 2×10^{-10} s^{-1}, which is far different than the experimental value of $(9.9 \pm 0.2) \times 10^{-3}$ s^{-1}, and the reason for this difference remains unclear.[6]

The decomposition of formyl chloride in aqueous solution[19] was found to decompose very rapidly into CO + HCl with a rate constant of about 10^4 s^{-1} and a half-life of about 7×10^{-5} s. This study also estimated that the decomposition of $CHCl_2$-(OH) took place with $t_{1/2} < 20$ μs in aqueous solution,[19] which is much faster than the value of $t_{1/2} = 126$ s found from the rate constant of $(5.5 \pm 0.3) \times 10^{-3}$ s^{-1} measured in the gas phase.[6] The decomposition of formyl chloride into CO + HCl products was also measured in the gas phase, and lifetimes were estimated to be 10 min in a 0.1 dm^3 reaction container[20] to between 28 and 190 min in a 480 dm^3 reaction container.[21] These experimental results are similar to those found for the gas phase lifetimes of chloromethanols[5,6] and also suggest that there is a heterogeneous component to the formyl chloride decomposition reaction. Quantum mechanical calculations for the spontaneous homogeneous decomposition of formyl chloride into CO + HCl products estimated a barrier of 43.95 kcal/mol and a lifetime on the order of 10^{13} years,[22] which is far too long as compared to the experimental gas phase lifetimes of

* To whom correspondence should be addressed. (D.L.P.) Tel: 852-2859-2160. Fax: 852-2857-1586. E-mail: phillips@hkucc.hku.hk. (C.Z.) Tel: 86-8411-0696. E-mail: ceszhcy@sysu.edu.cn.

† The University of Hong Kong.

‡ Sun Yat-Sen University.

10.1021/jp053015y CCC: $30.25
Published on Web 09/30/2005

SCHEME 1

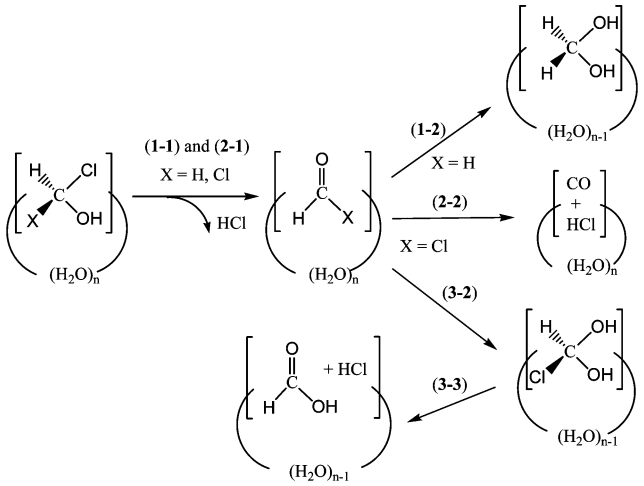

10−190 min[20,21] and the even shorter lifetime on the order of 10^{-4} s in aqueous solution.[19] The rate constant for the gas phase reaction of H_2O with formyl chloride (HClCO) was found to be faster[21] than the reaction of H_2O with Cl_2CO, which had an activation energy of 14 kcal/mol,[24] so one would expect that the activation energy for the reaction of H_2O with formyl chloride would be even smaller. Ab initio calculations for the reaction of H_2O with formyl chloride predicted a barrier of about 44 kcal/mol,[23] and this is too big as compared to the experimental value of <14 kcal/mol.[21,24] It was suggested that water may assist (or catalyze) these reactions.[23]

The discrepancies between the experimental and the calculated rates of decomposition of chlorinated methanols and formyl chloride in the gas phase and the much faster experimentally observed decomposition of these species in aqueous solutions prompted us to explore the decomposition of these species in the presence of water. In this paper, we report a systematic ab initio study of the chloromethanol, dichloromethanol, and formyl chloride reactions with water. We find that even the presence of one water molecule greatly accelerates the decomposition of chlorinated methanols and formyl chloride and these decomposition reactions are further accelerated as more water molecules are added to the reaction system. Rate constants for the decomposition of chlorinated methanols and formyl chloride from these ab initio studies are shown to be in reasonable agreement with experimental observations of aqueous phase decomposition reactions of dichloromethanol [$CHCl_2(OH)$] and formyl chloride and probably consistent with gas phase experimental results. We briefly describe the mechanism for the water catalysis of the decomposition reactions of these compounds and discuss probable implications for the decomposition of these chlorinated methanol compounds and formaldehydes in the natural environment and in advanced oxidation processes for the treatment of drinking water.

II. Computational Details

Second-order Møller−Plesset perturbation theory (MP2) was used to investigate the gas phase and water-assisted reaction mechanisms of the decomposition of chloromethanol [$CH_2Cl(OH)$] and dichloromethanol [$CHCl_2(OH)$] in both the gas phase and an aqueous solution. We have considered three major types of reactions (see Scheme 1). The first reaction type involves the decomposition of $CH_2Cl(OH)$ to formaldehyde (HCHO) and hydrogen chloride (HCl) in the gas phase and in water (reaction 1-1) followed by the hydration of the formaldehyde in water to produce its diol [$CH_2(OH)_2$] (reaction 1-2) as shown below.

$$CH_2(OH)Cl + nH_2O \rightarrow HCHO + nH_2O + HCl \ (n = 0, 1, 2, ..., 6) \quad (1\text{-}1)$$

$$HCHO + nH_2O \rightarrow CH_2(OH)_2 + (n-1)H_2O \ (n = 1, 2, ..., 4) \quad (1\text{-}2)$$

These may be added together to obtain the first overall reaction 1 given below:

$$CH_2(OH)Cl + 2nH_2O \rightarrow CH_2(OH)_2 + HCl + (2n-1)H_2O \quad (1)$$

The second type of reaction is the decomposition of $CHCl_2(OH)$ to formyl chloride (ClCHO) and hydrogen chloride (HCl) in the gas phase and in water (reaction 2-1) followed by decomposition of formyl chloride into CO and HCl in the gas phase and in water (reaction 2-2) as shown below.

$$CH(OH)Cl_2 + nH_2O \rightarrow ClCHO + nH_2O + HCl \ (n = 0, 1, 2, ..., 6) \quad (2\text{-}1)$$

$$ClCHO + nH_2O \rightarrow CO + HCl + nH_2O \ (n = 0, 1, 2, ..., 4) \quad (2\text{-}2)$$

These two reactions may be added together to obtain the second overall reaction 2 shown below:

$$CH(OH)Cl_2 + 2nH_2O \rightarrow CO + HCl + (2n)H_2O \quad (2)$$

The third type of reaction is the decomposition of $CHCl_2(OH)$ into formyl chloride (ClCHO) and hydrogen chloride (HCl) in the gas phase and in water (note that reaction 3-1 is same as reaction 2-1) followed by the hydration of the formyl chloride in water to produce chloromethanol diol [$CHCl(OH)_2$] (reaction 3-2). This reaction then proceeds by decomposition of $CHCl(OH)_2$ into formyl acid (HCOOH) and HCl in water (reaction 3-3) as shown below.

$$CH(OH)Cl_2 + nH_2O \rightarrow ClCHO + nH_2O + HCl \ (n = 0, 1, 2, ..., 6) \quad (3\text{-}1)$$

$$ClCHO + nH_2O \rightarrow CH(Cl)(OH)_2 + (n-1)H_2O \ (n = 1, 2, ..., 4) \quad (3\text{-}2)$$

$$CH(OH)_2Cl + nH_2O \rightarrow HCOOH + HCl + nH_2O \ (n = 0, 1) \quad (3\text{-}3)$$

These three reactions may be added to obtain the third overall reaction 3 as indicated below:

$$CH(OH)Cl_2 + 3nH_2O \rightarrow HCOOH + 2HCl + (3n-1)H_2O \quad (3)$$

We have considered the effect of water solvent on the reactions by explicitly adding water one by one into the reactant complexes (RCs) or the water-solvated clusters. The clusters consist of reactants $CH_2(OH)Cl$ or $CH(OH)Cl_2$ molecules and one, two, three, four, five, and six water molecules for reactions 1-1 and 2-1 or 3-1. The reactions 1-2, 2-2, and 3-2 were considered for up to four water molecules, in which one water molecule is the reactant and all of the other water molecules

can be regarded as catalysts. The reaction 3-3 was only considered in gas phase (no water involved) and one water molecule.

All of the reactions have been investigated by optimizing the RC, transition states (TS), and product complexes (PC) with water clusters containing up to six water molecules. The structures of the RC, TS, and PC are denoted as $(RC)_{ijn}$, $(TS)_{ijn}$, and $(PC)_{ijn}$ in the following text, tables, and figures, where *i* represents the number of reactions, *j* represents the step of the reaction, and *n* is the number of water molecules in the reaction. For instance, $(RC)_{216}$ represents the reaction complex for the first step of the second reaction with six water molecules, i.e., the reaction complex of $CH(OH)Cl_2 + 6H_2O \rightarrow ClCHO + 6H_2O + HCl$.

Stationary structures for all RC, TS, and PC were fully optimized without symmetry constraints (C_1 symmetry). The standard 6-31+G** basis set was employed in both optimization and frequency calculations. Five-component d functions were used in all calculations. Analytical frequency calculations were performed in order to confirm the optimized structures to be either a minimum or a first-order saddle-point as well as to obtain the zero-point energy correction for the reactions containing less than four water molecules. The frequency calculations for the reaction systems containing five and six water molecules were performed numerically due to limited computer resources for the MP2 frequency calculations. IRC calculations[25] were performed for part of the reaction systems to confirm that the optimized TS correctly connects the relevant reactants and products. The three main types of reactions include 29 subreactions containing different water molecules. Therefore, a total of 87 stationary structures for RC, TS, and PC were located.

To compare with the experimental gas phase and solution phase kinetics data available in the literature, the energies of the stationary structures for reactions 1-1, 2-1, and 2-2 were refined by single-point calculations done at the MP2 level of theory using a larger basis set aug-cc-pVDZ. In addition to the explicit coordination of solvent water molecules to the reactions, bulk solvation effects were also examined with the polarized continuum solvation model (D-PCM)[26] (implemented in the latest version of Gaussian 03) utilized for water ($\epsilon = 78.39$) and applied to reactions 1-1, 2-1, and 2-2. The activation free energy in the presence of water solvent, noted $\Delta G^{\ddagger}_{solv}$, was evaluated as $\Delta G^{\ddagger}_{solv} = \Delta G^{\ddagger}_{gas} + \Delta\Delta G^{\ddagger}_{solv}$, where $\Delta G^{\ddagger}_{gas}$ is the activation free energy at the MP2/aug-cc-pVDZ level of theory and $\Delta\Delta G^{\ddagger}_{solv}$ is defined as the difference between the solvation energy of RC and TS from the B3LYP/aug-cc-pVDZ calculations. Bondi's atomic radii[27] were used in the D-PCM calculations, in which hydrogen atoms were explicitly considered to build up the solvation cavity. The utilization of Bondi radii is advantageous because these radii are obtained from crystallographic data and appear more reasonable for condensed phase environments. Moreover, the explicit hydrogen atom consideration in the model appears reasonable for modeling the solvation process for the water-assisted hydrogen transfer reactions studied here. We also note that a very recent paper reported a successful prediction of the absolute pK_a values of organic acids in dimethyl sulfoxide solution by using a PCM−Bondi model.[28] All calculations were carried out using the Gaussian 98 and Gaussian 03 program suites.[29] To validate the utilization of B3LYP/aug-cc-pVDZ-DPCM-BONDI level for calculating $\Delta\Delta G^{\ddagger}_{solv}$, we have performed a comparison calculation for the smaller reaction system (2-2) at both MP2 and B3LYP levels. It is found that the two levels can predict very similar results (see Figure 9 for details). Therefore, we believe that the current MP2/ MP2/aug-cc-pVDZ (gas) + B3LYP/aug-cc-pVDZ-DPCM-BONDI (solution) model can provide a good estimation of activation free energies for the aqueous solution reactions studied here. Furthermore, to mimic a real aqueous environment for the reactions, we have proposed a simple model to explain the water catalysis between experiment and theory. The model is described in detail in section D.

III. Results and Discussion

The optimized stationary structures (minima, saddle points) on the potential energy surfaces of the reactions studied here are depicted schematically in Figures 1−5. Selected key geometry parameters (bond lengths given in Å) are also shown in these figures. The detailed structural parameters and energies for the structures determined in this study are collected in the Supporting Information. The relative energies including ZPE for the different reactions examined here are shown graphically in Figure 6a−c. The calculated thermodynamic and kinetic parameters for the reactions are tabulated in Tables 1 and 2. The relationship between the reaction barriers ($\Delta E^{\ddagger}$) and the stabilization energies of the RC and the PC (ΔE_{RC}, ΔE_{PC}) relative to separated reactants and products are shown in Figures 7a−c and 8a,b as a function of the number of water molecules in the cluster.

A. Decomposition Reactions of Chloromethanol in the Gas Phase and in Aqueous Solution. *1. $CH_2(OH)Cl + nH_2O \rightarrow HCHO + HCl + nH_2O$ (Where n = 0, 1, 2, 3, 4, 5, 6).* Figure 1 displays the optimized geometry found for the reactions of $CH_2Cl(OH) + nH_2O \rightarrow HCHO + HCl + nH_2O$, i.e., $(RC)_{11n} \rightarrow (TS)_{11n} \rightarrow (PC)_{11n}$ where $n = 0, 1, 2, 3, 4, 5, 6$. Examination of Figure 1 shows that the gas phase homogeneous decomposition reaction of $CH_2Cl(OH) \rightarrow HCl + HCHO$ proceeds through the four-centered cyclic $(TS)_{110}$ where the Cl atom is almost detached from the carbon atom (the C−Cl bond is elongated from 1.797 to 2.586 Å) and approaches the hydrogen atom in the $CH_2Cl(OH)$ H−O bond (the distance of H···Cl is 2.007 Å, and the HCl molecule is partially formed in the TS). The four-centered TS is similar to that proposed by Wallington and coworkers in the gas phase homogeneous decomposition reaction of $CCl_3(OH) \rightarrow HCl + Cl_2CO$.[6] In the one and two water catalytic reactions, the water molecules are incorporated into the leaving group H···Cl through cyclic hydrogen bonds, i.e., $(O)H[(CH_2Cl(OH)]\cdots O-H(H_2O)_n$ ($n = 1, 2$)···Cl for $(RC)_{11n}$, $(TS)_{11n}$, and $(PC)_{11n}$ ($n = 1, 2$). It is worth noting that there exist systematic structural changes in going from the RC to the corresponding TS and PC for $(RC)_{11n} \rightarrow (TS)_{11n} \rightarrow (PC)_{11n}$ where $n = 0, 1, 2$. For instance, the H−O bonds [0.967 Å for $(RC)_{110}$, 0.975 Å for $(RC)_{111}$, and 0.979 Å for $(RC)_{112}$] and the C−Cl bonds [1.797 Å for $(RC)_{110}$, 1.822 Å for $(RC)_{111}$, and 1.838 Å for $(RC)_{112}$] become systematically elongated for the $(RC)_{11n}$ as the number of water molecules (*n*) increases from 0 to 2. Meanwhile, the distances for the leaving group H···Cl become shorter [2.860 Å for $(RC)_{110}$, 2.815 Å for $(RC)_{111}$, and 2.671 Å for $(RC)_{112}$]. The systematic elongation of the C−Cl bonds and the shortening of the weak H···Cl interactions for the RC suggest that there is a systematic trend for activating the C−Cl bonds and partial formation of the H−Cl leaving group as the number of water molecules ($n = 0, 1, 2$) are explicitly incorporated to the reaction systems. The H−O bonds become elongated from 1.030 Å for $(TS)_{110}$ to 1.290 Å for $(TS)_{111}$ and 1.362 Å for $(TS)_{112}$, indicating that H_3O^+ or $H_5O_2^+$ ions become almost formed in the $(TS)_{111}$ and $(TS)_{112}$. We note that the $(TS)_{111}$ and $(TS)_{112}$ are greatly stabilized by

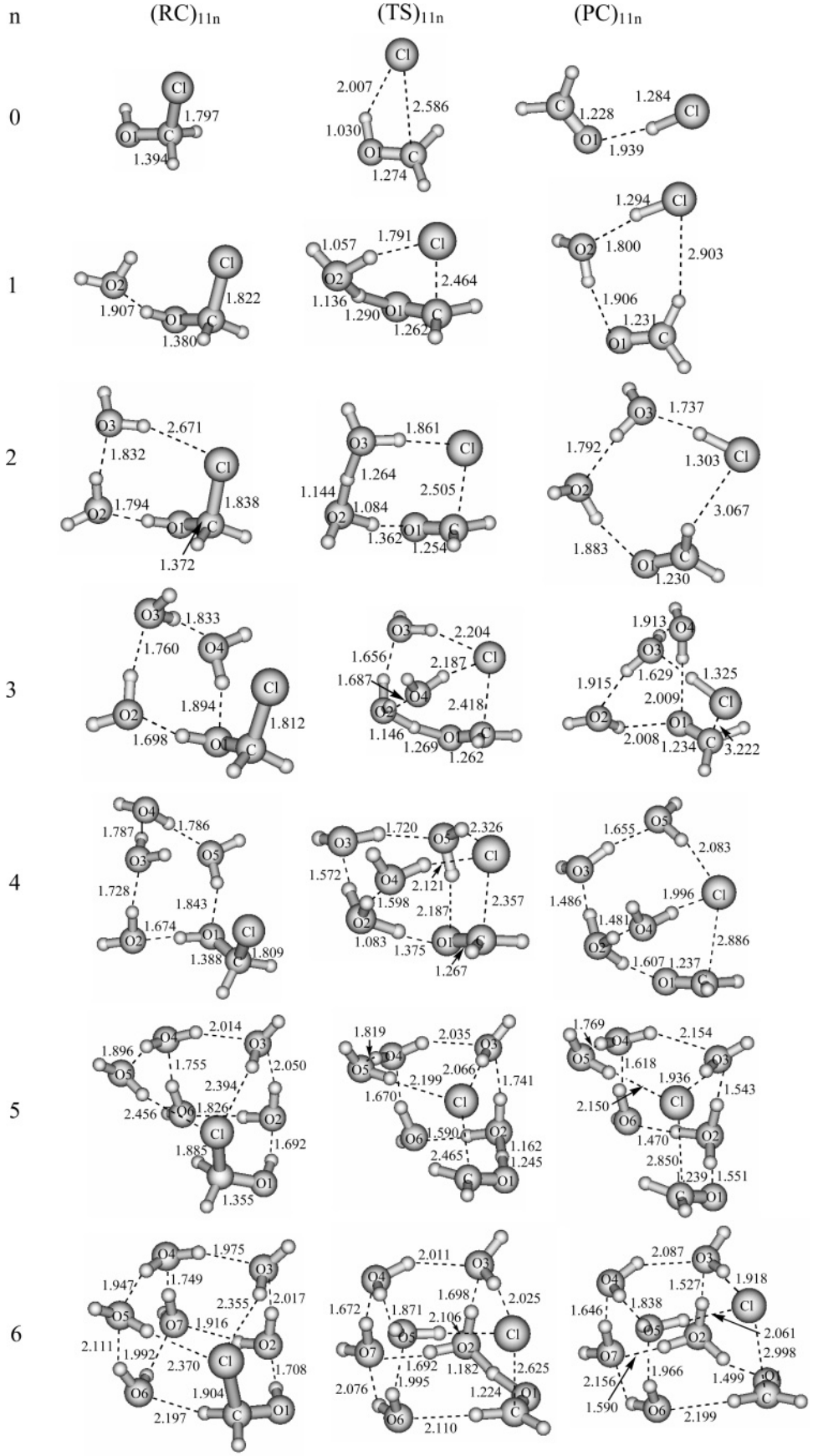

Figure 1. Optimized geometry (bond lengths are in Angstroms) for all of the reactants, RC, TS, and PC obtained from the MP2/6-31+G** calculations are shown for the $CH_2(OH)Cl + nH_2O \rightarrow HCHO + nH_2O + HCl$ ($n = 0, 1, 2, ..., 6$) reactions [associated with structures $(RC)_{11n}$, $(TS)_{11n}$, and $(PC)_{11n}$ where $n = 0, 1, 2, 3, 4, 5, 6$].

the H_3O^+ Cl^- and $H_5O_2^+$ Cl^- pairs, in which the H···Cl interactions are stronger than that in the gas phase reaction (e.g., smaller H···Cl distances than that in the gas phase). However, in the $(PC)_{110}$, $(PC)_{111}$, and $(PC)_{112}$, the zwitterions $H_3O^+Cl^-$

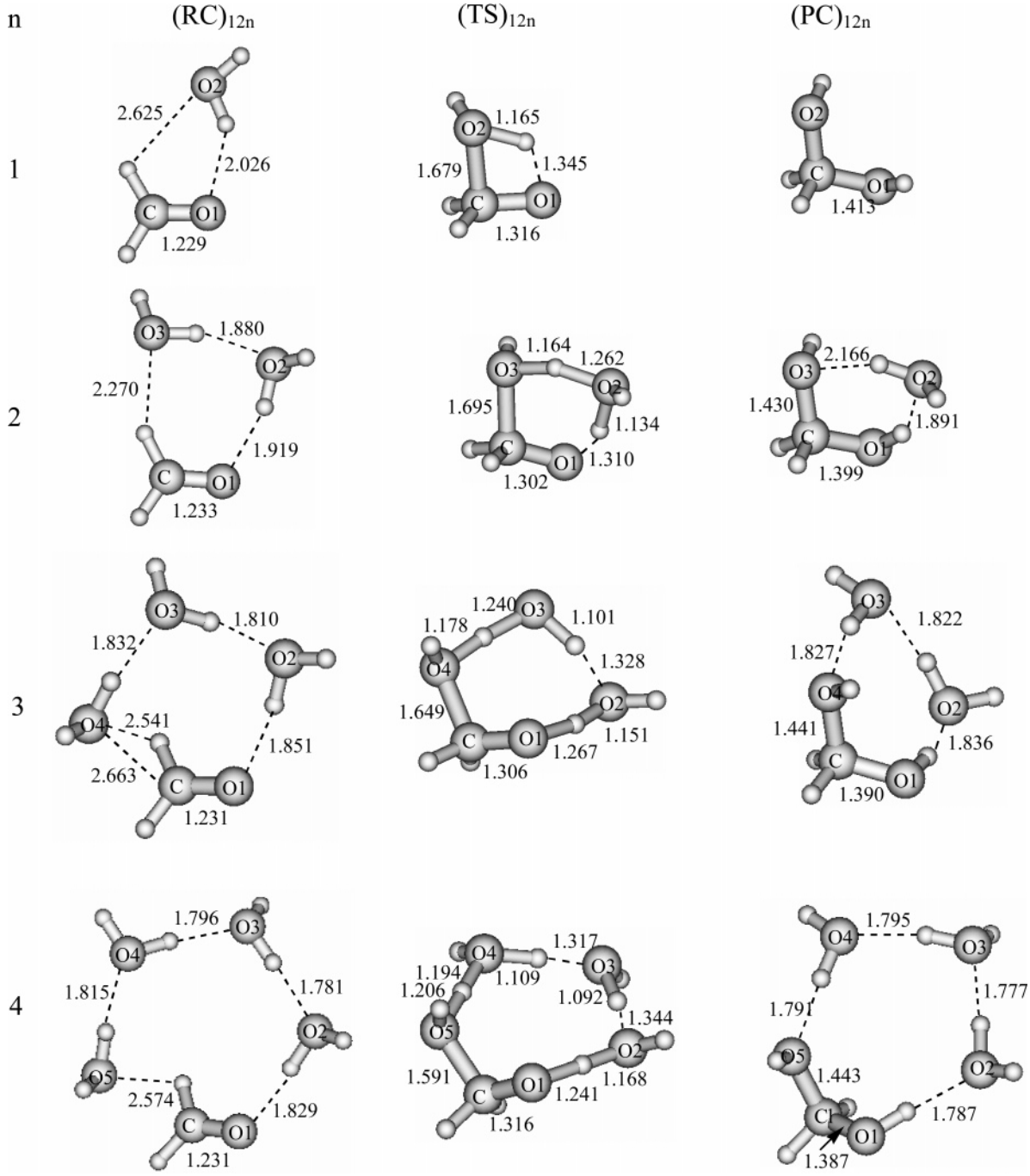

Figure 2. Optimized geometry (bond lengths are in Angstroms) for all of the reactants, RC, TS, and PC obtained from the MP2/6-31+G** calculations are shown for the $HCHO + nH_2O \rightarrow CH_2(OH)_2 + (n-1)H_2O$ ($n = 1, 2, ..., 4$) reactions [associated with structures $(RC)_{12n}$, $(TS)_{12n}$, and $(PC)_{12n}$ where $n = 1, 2, 3, 4$].

and $H_5O_2^+Cl^-$ will collapse and associate to produce HCl and H_2O molecules.

For the three and four water catalytic reactions, it can be seen from Figure 1 that cyclic hydrogen bonds are formed with three or four water oxygen atoms (O2, O3, O4, or O5) and the CH_2-Cl(OH) oxygen atom (O1) for $(RC)_{113}$ and $(RC)_{114}$. The RC show a different hydrogen bond mode as compared to the one and two water-involved reactions, in which the cyclic hydrogen bonds are formed with the C−O1, O2, O3, and Cl atoms. The C−Cl bonds with lengths of 1.812 Å for $(RC)_{113}$ and 1.809 Å for $(RC)_{114}$ are only slightly elongated as compared to that in $CH_2Cl(OH)$ since no H···Cl weak interactions are involved for these RCs. The most intriguing feature is that the cagelike TS are formed for $(TS)_{113}$ and $(TS)_{114}$, in which three or four different types of cyclic hydrogen bonds are formed, i.e., the cyclic hydrogen bonds Cl···CO1···O2···O3···Cl, Cl···CO1···O2···O4···Cl, and Cl···O3···O2···O4···Cl for $(TS)_{113}$ and Cl···CO1···O2···O4···Cl, Cl···O4···O2···O3···O5···Cl, Ol···O2···O3···O5···O1, and Cl···CO1···O5···Cl for $(TS)_{114}$, respectively (the hydrogen atoms are omitted for clarification). It is interesting to note that in $(TS)_{113}$ and $(TS)_{114}$, the leaving Cl atoms are stabilized by two H···Cl interactions. This suggests that there is a greater stabilization for these TS structures as compared to those for the gas phase and the smaller water cluster ($n = 0$, 1, 2)-involved reactions. We shall discuss the energetics of these reactions in subsequent sections.

The cubic water octamer has been well-studied both experimentally[30,31] and theoretically[32−34] and found to be the most

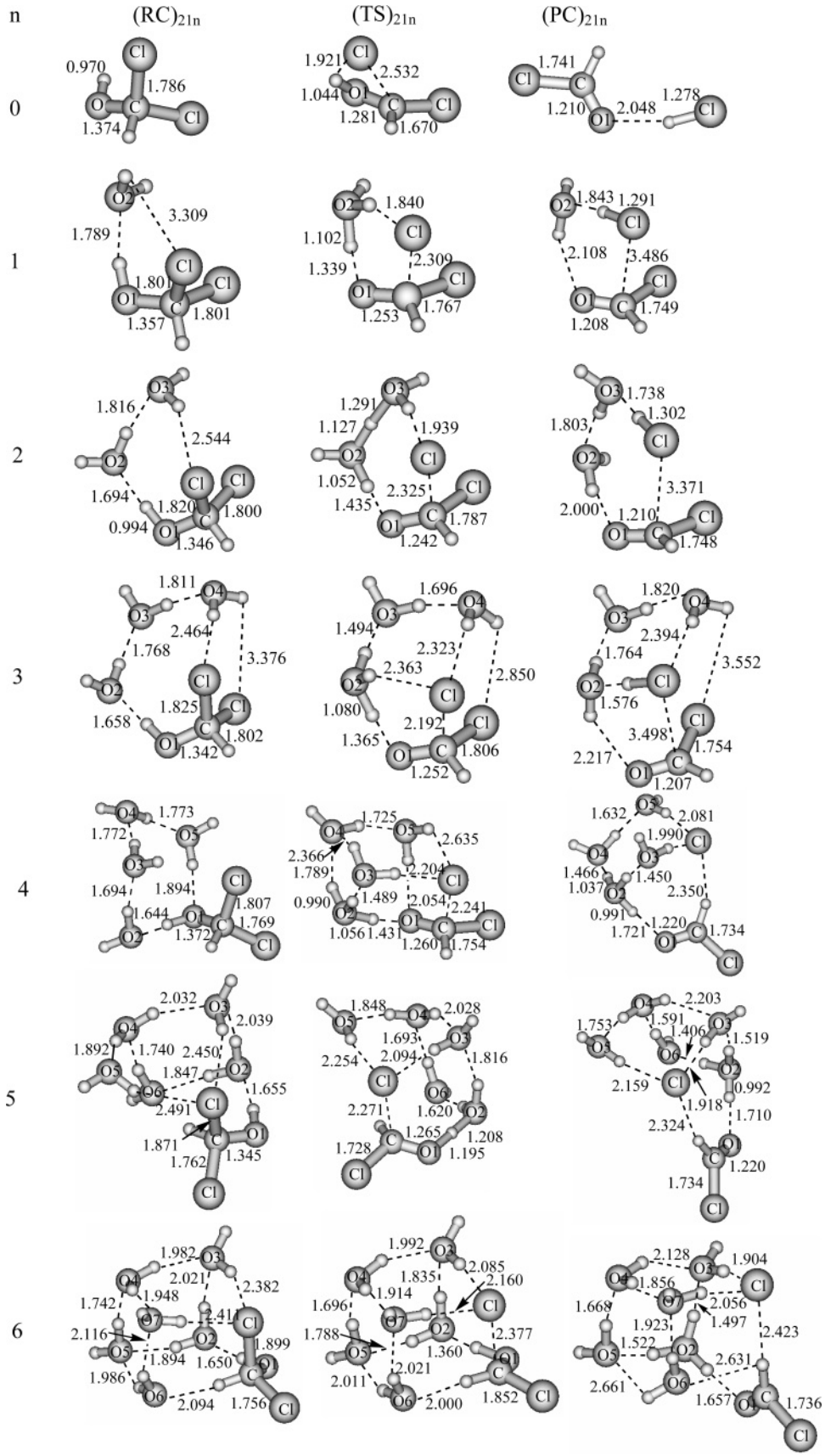

Figure 3. Optimized geometry (bond lengths are in Angstroms) for all of the reactants, RC, TS, and PC obtained from the MP2/6-31+G** calculations are shown for the $CH(OH)Cl_2 + nH_2O \rightarrow ClCHO + nH_2O + HCl$ ($n = 0, 1, 2, ..., 6$) reactions [associated with structures $(RC)_{21n}$, $(TS)_{21n}$, and $(PC)_{21n}$ where $n = 0, 1, 2, 3, 4, 5, 6$].

stable neutral water clusters with a much larger binding energy (per water molecule) than those of the hexamer and heptamer water clusters.[34] To build larger water cluster-catalyzed reactions, six water molecules were incorporated into the reactant molecule $CH_2Cl(OH)$ to form a cubic structure, in which six water molecules occupy six corners of the cube while the Cl

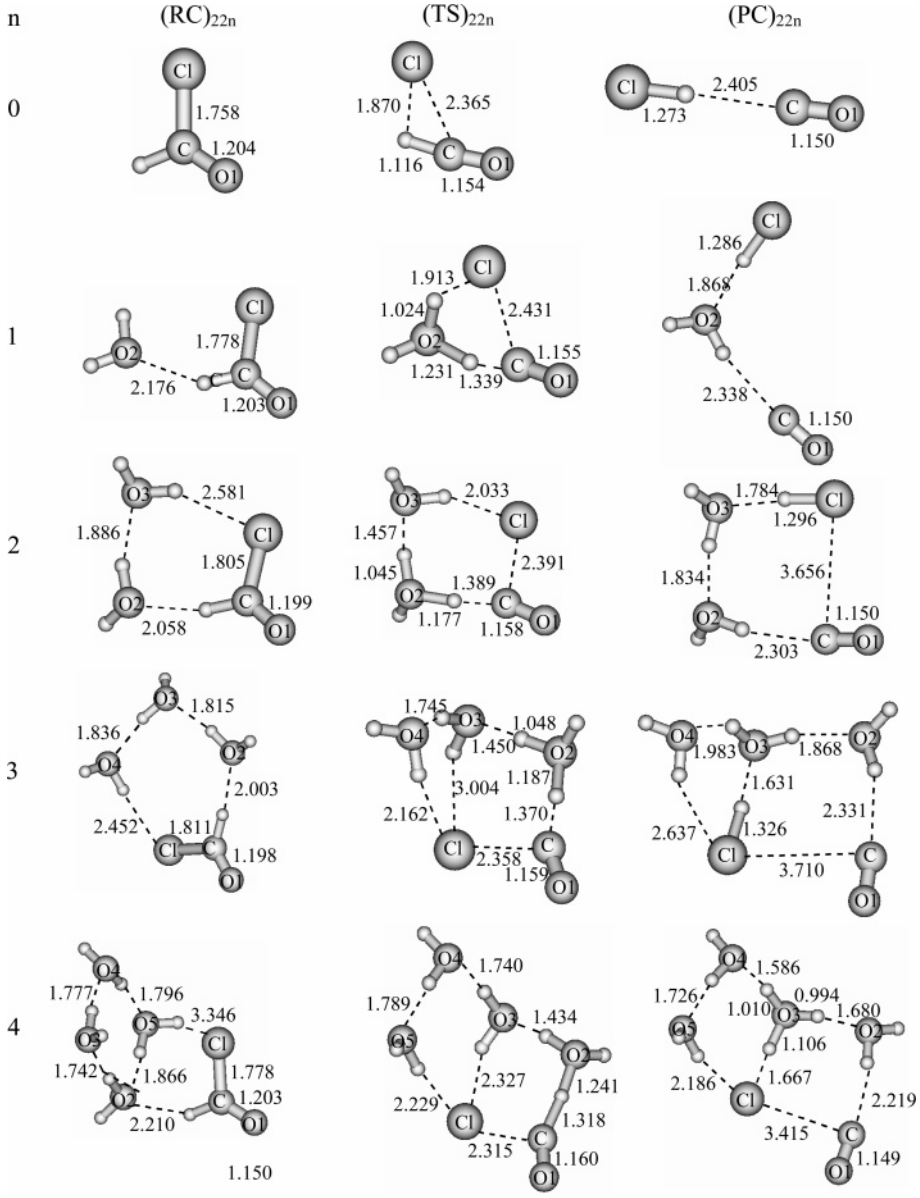

Figure 4. Optimized geometry (bond lengths are in Angstroms) for all of the reactants, RC, TS, and PC obtained from the MP2/6-31+G** calculations are shown for the $ClCHO + nH_2O \rightarrow CO + HCl + nH_2O$ ($n = 0, 1, 2, ..., 4$) reactions [associated with structures $(RC)_{22n}$, $(TS)_{22n}$, and $(PC)_{22n}$ where $n = 0, 1, 2, 3, 4$].

atom and the CH_2OH moiety of $CH_2Cl(OH)$ occupy the other two corners. In this cubic RC, the Cl atom is stabilized by two H···Cl interactions. This is different from the smaller water-solvated RC as n goes from 0 to 4 in which only one or no interaction occurs between H and Cl. In addition, the leaving H atom in the OH moiety of $CH_2Cl(OH)$ is hydrogen-bonded to the neighboring water O2 atom while the H atom in the CH_2 group is weakly bonded to the neighboring water O6 atom to form a C−H···O hydrogen bond. All of the other water molecules are connected to each other with H···O hydrogen bonds. Inspection of Figure 1 shows that as the $(RC)_{116}$ goes to $(TS)_{116}$, the Cl atom becomes detached from the C atom while the Cl atom is stabilized by two neighboring hydrogen atoms and become closer together as compared to those in $(RC)_{116}$. Another interesting feature is that the H atom in the OH moiety of $CH_2Cl(OH)$ is shared by the $CH_2Cl(OH)$ O1 atom and the H_2O O2 atom. It appears that the degree of elongation of the C−Cl bond from $(RC)_{116}$ to $(TS)_{116}$ is greater than those of the other water-solvated reaction systems where $n = 0-4$. However, the two stronger H···Cl interactions (the shortening of H···Cl distances from RC to TS are as large as 0.26 and 0.33 Å) would help compensate the energy needed for cleavage of the C−Cl bond. In addition, there is a smaller structural change for the six-water solvated clusters in going from $(RC)_{116}$ to $(TS)_{116}$ as a whole as compared to the large structural rearrangement of the water clusters for the smaller water cluster-solvated reactions where $n = 0-4$ since the hydrogen bond network of the six-water solvated cubic structure will not change too much upon going from the RC to the TS. The five water catalytic reaction has structural features similar to the six-water solvated cubic structure except for one corner of the water cubic cluster missing from the cluster.

It should be noted that there are some general trends for the structural features of the PC. Most of the PC geometries are quite similar to the corresponding TS geometries. In the case of $n = 0-3$, the proton is transferred from the H_3O^+ and $H_5O_2^+$ like moiety to form the associated neutral HCl molecule. However, in the case of $n = 4-6$, the $H_3O^+Cl^-$ pairs of PCs retain the same configuration as that in the corresponding TS. As the number of water molecules increases from $n = 0$ to 4,

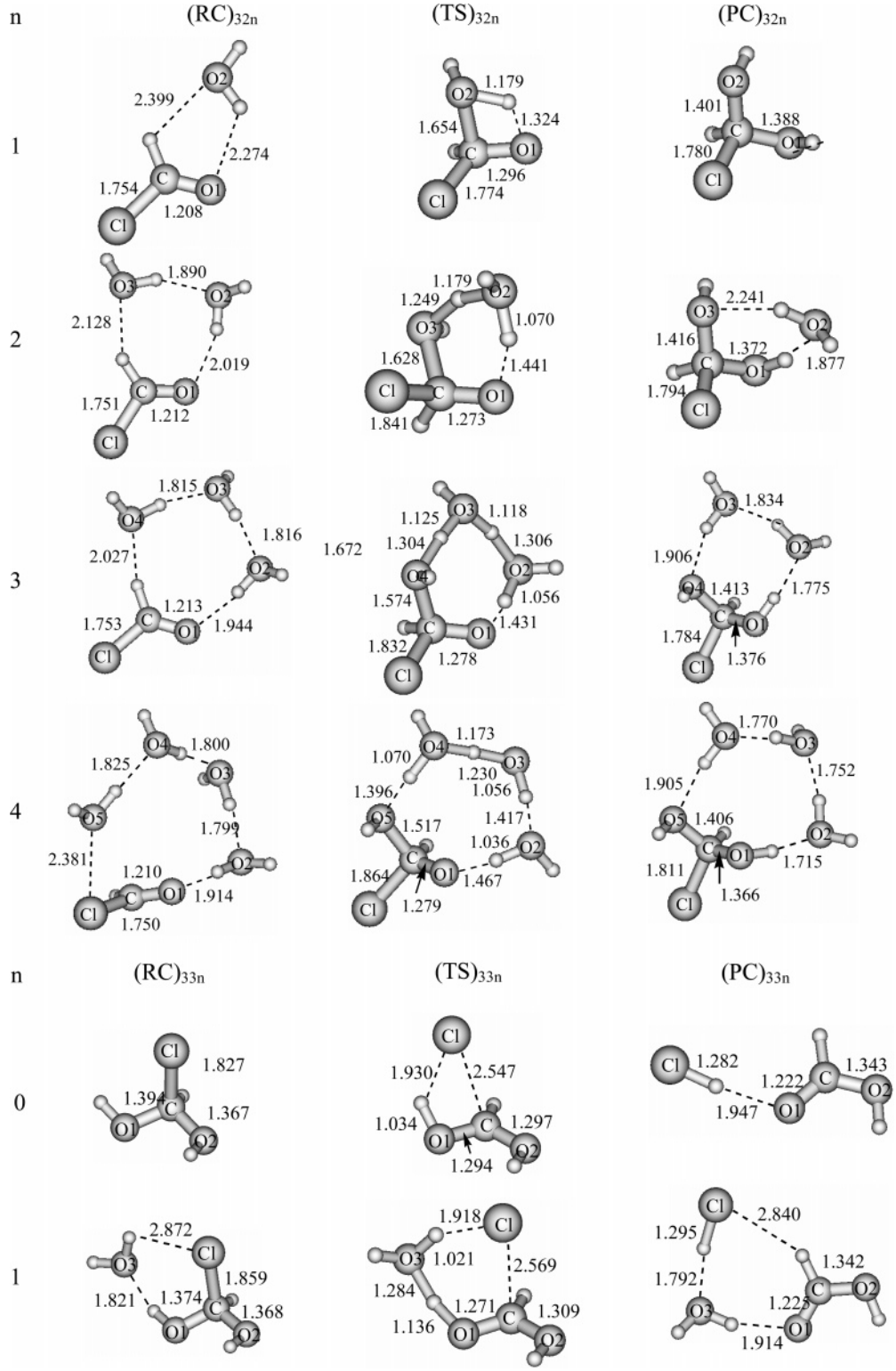

Figure 5. Optimized geometry (bond lengths are in Angstroms) for all of the reactants, RC, TS, and PC obtained from the MP2/6-31+G** calculations are shown for the $ClCHO + nH_2O \rightarrow CH(Cl)(OH)_2 + (n-1)H_2O$ ($n = 1, 2, ..., 4$) and $CH(OH)_2Cl + nH_2O \rightarrow HCOOH + HCl + nH_2O$ ($n = 0, 1$) reactions [associated with structures $(RC)_{32n}$, $(TS)_{32n}$, and $(PC)_{32n}$ where $n = 1, 2, 3, 4$ and $(RC)_{33n}$, $(TS)_{33n}$, and $(PC)_{33n}$ where $n = 0, 1$, respectively].

the HCl bond length becomes systematically elongated from 1.284 Å for $(PC)_{110}$ in the gas phase to 1.294 Å for $(PC)_{111}$, 1.303 Å for $(PC)_{112}$, and 1.325 Å for $(PC)_{113}$, and a separated $H_3O^+Cl^-$ pair is found for $(PC)_{114}$. This is quite similar to the changes observed in the dissociation process of $HCl(H_2O)_n$ clusters.[36−39] The only difference is that one of the product HCHO molecules is replaced by a H_2O molecule; that is, the PC can be regarded as $HCl(HCHO)(H_2O)_n$ clusters.

In summary, the homogeneous decomposition reaction of $CH_2Cl(OH) \rightarrow HCl + HCHO$ in a water-solvated environment appears to take place by three major processes. In the case of $n = 1, 2$, the reactions can be regarded as two-dimensional (2D) cyclic model reactions, in which all of the RC, TS, and PC have similar cyclic configurations. In the case of $n = 3, 4$, the reactions can be regarded as the transition from the 2D to the three-dimensional (3D) solvated reaction models, in which the

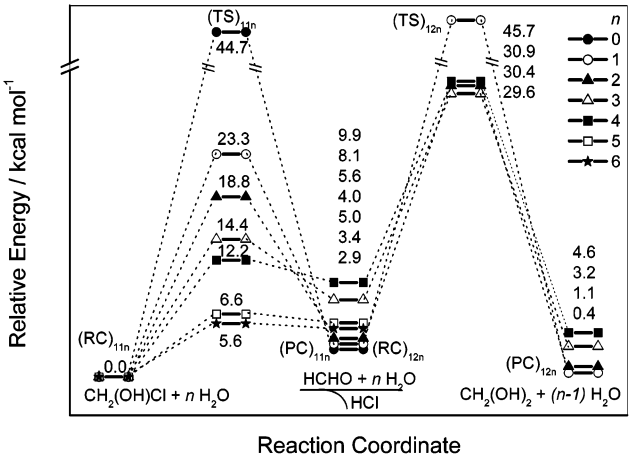

(a) **(1-1)** $CH_2(OH)Cl + nH_2O \rightarrow HCHO + nH_2O + HCl$
(1-2) $HCHO + nH_2O \rightarrow CH_2(OH)_2 + (n\text{-}1)H_2O$

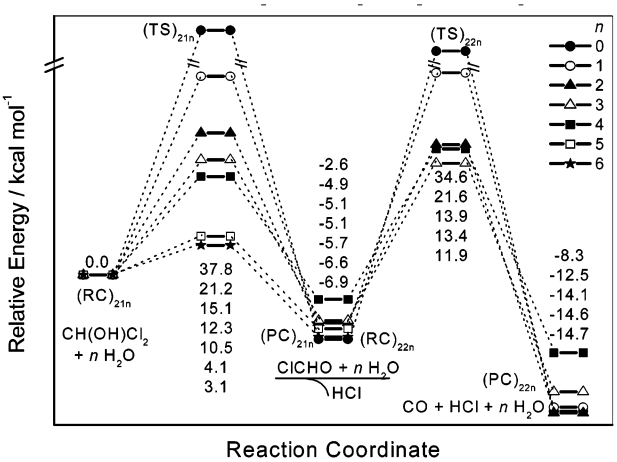

(b) **(2-1)** $CH(OH)Cl_2 + nH_2O \rightarrow ClCHO + nH_2O + HCl$
(2-2) $ClCHO + nH_2O \rightarrow CO + HCl + nH_2O$

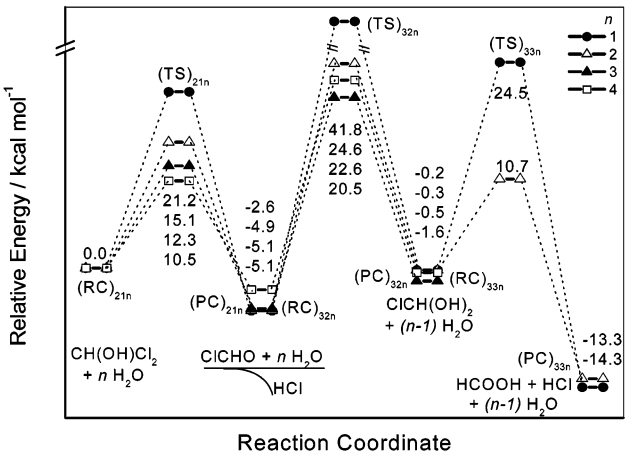

(c) **(3-1)** $CH(OH)Cl_2 + nH_2O \rightarrow ClCHO + nH_2O + HCl$
(3-2) $ClCHO + nH_2O \rightarrow CH(Cl)(OH)_2 + (n\text{-}1)H_2O$
(3-3) $CH(OH)_2Cl + nH_2O \rightarrow HCOOH + HCl + nH_2O$

Figure 6. (a) Relative energy profiles (in kcal/mol) obtained from MP2/6-31+G** ab initio calculations to study the $CH_2(OH)Cl + nH_2O \rightarrow HCHO + nH_2O + HCl$ ($n = 0, 1, 2, ..., 6$) and $HCHO + nH_2O \rightarrow CH_2(OH)_2 + (n-1)H_2O$ ($n = 1, 2, ..., 4$) reactions associated with structures $(RC)_{11n}$, $(TS)_{11n}$, and $(PC)_{11n}$ where $n = 0, 1, 2, 3, 4, 5, 6$ and $(RC)_{12n}$, $(TS)_{12n}$, and $(PC)_{12n}$ where $n = 1, 2, 3, 4$, respectively, that are shown in Figures 1 and 2. (b) Relative energy profiles (in kcal/mol) obtained from MP2/6-31+G** ab initio calculations to study the $CH(OH)Cl_2 + nH_2O \rightarrow ClCHO + nH_2O + HCl$ ($n = 0, 1, 2, ..., 6$) and $ClCHO + nH_2O \rightarrow CO + HCl + nH_2O$ ($n = 0, 1, 2, ..., 4$) reactions associated with structures $(RC)_{21n}$, $(TS)_{21n}$, and $(PC)_{21n}$ where $n = 0, 1, 2, 3, 4, 5, 6$ and $(RC)_{22n}$, $(TS)_{22n}$, and $(PC)_{22n}$ where $n = 0, 1, 2, 3, 4$, respectively, that are shown in Figures 3 and 4. (c) Relative energy profiles (in kcal/mol) obtained from MP2/6-31+G** ab initio calculations to study the $CH(OH)Cl_2 + nH_2O \rightarrow ClCHO + nH_2O + HCl$ ($n = 1, 2, ..., 4$); $ClCHO + nH_2O \rightarrow CH(Cl)(OH)_2 + (n-1)H_2O$ ($n = 1, 2, ..., 4$); and $CH(OH)_2Cl + (n-1)H_2O \rightarrow HCOOH + HCl + (n-1)H_2O$ ($n = 1, 2$) reactions associated with structures $(RC)_{21n}$, $(TS)_{21n}$, and $(PC)_{21n}$ where $n = 1, 2, 3, 4$; $(RC)_{32n}$, $(TS)_{32n}$, and $(PC)_{32n}$ where $n = 1, 2, 3, 4$; and $(RC)_{33n}$, $(TS)_{33n}$, and $(PC)_{33n}$ where $n = 0, 2$, respectively, that are shown in Figures 3 and 5.

TS and PC proceed to become cagelike 3D structures. This process can be regarded as a partially solvated model reaction. In the case of $n = 5$ and 6, the reactions can be regarded as a fully solvated 3D reaction system (just for the first water solvent shell), in which all of the RC, TS, and PC have cubic or cubiclike structures. The cubiclike water-solvated reaction model is the most efficient reaction pathway in the solution phase, and we shall discuss the energetics of these reactions in detail later.

To examine the charge distribution of the atoms in going from RC to TS and PC, natural orbital analyses were performed for most of the stationary structures. The charge for the Cl atoms in the RC $(RC)_{11n}$ is only slightly negative (from -0.12 to -0.20) while the charge of Cl atoms becomes much more negative (from -0.66 to -0.78) for the corresponding TS $(TS)_{11n}$ where $n = 0, 1, 2$. This suggests that a large amount of charge redistribution occurs upon going from the RC to their associated TS.

Inspection of Table 1 and Figure 6a shows that the gas phase decomposition reaction of $CH_2Cl(OH) \rightarrow HCl + HCHO$ has an activation barrier of 44.7 kcal/mol and is endothermic by about 4.1 kcal/mol. This predicted endothermicity of the decomposition reaction for chloromethanol is slightly smaller than the calculated ΔH(298.15 K) of 7.8 kcal/mol from MP2/6-311G(2d,p) calculations.[5] However, our calculated value is consistent with the experimental estimation of 2.3 ± 3 kcal/mol.[5] The activation Gibbs free energy and Gibbs free energy are computed to be 44.5 and 0.9 kcal/mol, respectively, giving a rate constant of 1.02×10^{-20} s^{-1} and a half-life time of 6.8×10^{19} s. The very large enthalpy of activation, small rate constant, and long lifetime for the decomposition of $CH_2Cl(OH) \rightarrow HCl + HCHO$ suggest that the reaction is unlikely to

TABLE 1: MP2/6-31+G(d, p) Calculated Energies ($\Delta E^{\ddagger}$, ΔE) (kcal mol^{-1}), Enthalpy ($\Delta H^{\ddagger}$, ΔH) (kcal mol^{-1}), Free Energies ($\Delta G^{\ddagger}$, ΔG) (kcal mol^{-1}), Entropy ($\Delta S^{\ddagger}$, ΔS) (cal mol^{-1} K^{-1}), Rate Constant (k) (s^{-1}), and Zero-Point Energies Difference between RC and TS (ΔZPE) (kcal mol^{-1}), Stabilization Energies of RC and PC (ΔE^{RC}, ΔE^{PC}) (kcal mol^{-1}) Relative to Separated Species[a]

reaction	$\Delta E^{\ddagger}$ [b]	$\Delta H^{\ddagger}$ [c]	$\Delta G^{\ddagger}$ThinSpacec	$\Delta S^{\ddagger}$	k[d]	ΔZPE[e]	ΔE_{RC}[f]	ΔE_{PC}[f]	ΔE[g]	ΔH[g]	ΔG[g]	ΔS
1-1: $CH_2(OH)Cl + nH_2O \rightarrow HCHO + nH_2O + HCl$ ($n = 0, 1, 2, ..., 6$)												
110	44.72	44.68	44.51	0.56	1.45×10^{-20}	−2.34	0.00	−4.14	2.90	4.06	0.87	10.69
111	23.27	22.22	24.70	−8.35	4.85×10^{-6}	−3.47	−7.31	−10.90	3.45	4.28	1.78	8.39
112	18.79	17.32	21.12	−12.74	2.04×10^{-3}	−3.60	−15.38	−18.38	4.04	4.72	2.71	6.74
113	14.37	13.58	16.09	−8.43	9.94×10^{0}	−2.64	−25.68	−20.34	12.38	9.37	6.18	10.70
114	12.20	11.00	15.28	−14.36	3.90×10^{1}	−1.56	−33.66	−30.84	9.86	9.53	9.90	−1.24
115	6.57	5.08	9.03	−13.25	1.49×10^{6}	−1.84	−38.46	−39.85	5.65	4.60	7.43	−9.50
116	5.55	4.16	7.39	−10.81	2.37×10^{7}	−2.13	−46.76	−48.75	5.05	4.28	5.58	−4.38
1-2: $HCHO + nH_2O \rightarrow CH_2(OH)_2 + (n-1)H_2O$ ($n = 1, 2, ..., 4$)												
121	42.28	40.65	44.61	−13.30	1.23×10^{-20}	−0.43	−3.78	0.00	−3.01	−4.53	−0.72	−12.78
122	26.39	24.00	29.56	−18.65	1.33×10^{-9}	−0.45	−11.07	−7.15	−2.86	−4.21	−0.87	−11.22
123	21.57	18.61	25.72	−23.83	8.66×10^{-7}	−1.65	−19.10	−17.15	−4.84	−6.48	−2.32	−13.96
124	21.01	17.84	25.78	−26.62	7.83×10^{-7}	−2.78	−26.50	−24.96	−5.25	−6.62	−2.93	−12.39
2-1: $CH(OH)Cl_2 + nH_2O \rightarrow ClCHO + nH_2O + HCl$ ($n = 0, 1, 2, ..., 6$)												
210	37.86	37.84	37.62	0.74	1.64×10^{-15}	−2.72	0.00	−3.20	−6.86	−5.59	−9.78	14.07
211	21.19	20.17	22.79	−8.79	1.22×10^{-4}	−2.61	−8.24	−9.69	−5.12	−4.14	−7.28	10.52
212	15.13	14.03	16.38	−7.89	6.09×10^{0}	−2.58	−16.52	−17.95	−5.09	−4.04	−8.15	13.77
213	12.28	11.26	12.55	−4.30	3.92×10^{3}	−1.44	−24.10	−25.31	−4.87	−4.22	−6.18	6.56
214	10.49	9.61	11.14	−5.16	4.23×10^{4}	−0.88	−32.76	−31.70	−2.60	−2.85	−2.46	−1.31
215	4.11	3.08	4.96	−6.32	1.44×10^{9}	−1.89	−37.92	−40.00	−5.74	−6.50	−5.78	−2.39
216	3.14	1.91	4.90	−10.01	1.59×10^{9}	−0.46	−46.48	−49.47	−6.65	−7.17	−6.79	−1.29
2-2: $ClCHO + nH_2O \rightarrow CO + HCl + nH_2O$ ($n = 0, 1, 2, ..., 4$)												
220	41.46	41.72	41.05	2.26	5.00×10^{-18}	−3.16	0.00	−1.42	−7.70	−6.41	−6.62	0.71
221	26.68	25.36	29.13	−12.65	2.74×10^{-9}	−2.29	−3.90	−6.62	−9.00	−8.33	−10.95	8.80
222	18.97	17.54	21.19	−12.25	1.81×10^{-3}	−2.26	−10.26	−13.60	−9.63	−8.91	−11.28	7.96
223	16.77	15.37	19.29	−13.14	4.48×10^{-2}	−2.08	−17.74	−19.05	−7.59	−6.55	−9.90	11.24
224	16.02	15.17	18.41	−10.88	1.98×10^{-1}	−3.22	−28.09	−27.51	−5.70	−5.50	−5.57	0.23
3-2:[a] $ClCHO + nH_2O \rightarrow CH(Cl)(OH)_2 + (n-1)H_2O$ ($n = 1, 2, ..., 4$)												
321	46.97	45.23	49.99	−15.96	1.40×10^{-24}	−0.72	−3.98	0.00	4.90	3.24	7.90	−15.63
322	29.65	27.22	33.34	−20.51	2.25×10^{-12}	−0.28	−11.84	−7.93	4.83	3.44	7.35	−13.11
323	25.39	22.67	29.58	−23.18	1.28×10^{-9}	−1.18	−20.07	−17.68	3.32	1.92	5.97	−13.60
324	25.18	22.06	30.48	−28.24	2.81×10^{-10}	−0.97	−26.23	−25.09	2.06	0.47	4.54	−13.67
3-3: $CH(OH)_2Cl + nH_2O \rightarrow HCOOH + HCl + nH_2O$ ($n = 0, 1$)												
331	24.72	24.53	24.61	−0.27	5.64×10^{-6}	−1.77	0.00	−9.29	−14.14	−13.14	−16.66	11.81
332	11.04	10.01	12.41	−8.03	4.96×10^{-3}	−2.01	−8.03	−16.16	−12.98	−12.36	−14.76	8.05

[a] The reactions 3-1 are same as 2-1 and are omitted from the table. [b] $\Delta E^{\ddagger}$: Energies of activation for the reaction with ZPE correction. [c] $\Delta H^{\ddagger}$, $\Delta G^{\ddagger}$: Enthalpies and free energies of activation for the reaction. [d] k: calculated from free energy of activation, $\Delta G^{\ddagger}$. [e] ΔZPE = ZPE(TS) − ZPE(RC). [f] ΔE_{RC}, ΔE_{PC}: Stabilization energies for RC and PC relative to corresponding separated species with ZPE correction. [g] ΔE,ΔH, ΔG: Relative energies, enthalpies and free enegrgies for the reactions (between RC and PC).

TABLE 2: Calculated Activation Free Energies ($\Delta G^{\ddagger}$, kcal mol^{-1}), Rate Constant (k, s^{-1}) from Different Levels of Theory and Experimentally Observed Pseudo-First-Order Rate Constant (s^{-1}) in Gas Phase

	MP2/6-31+G**		MP2/aug-cc-pVDZ		QCISD(T)/aug-cc-pVDZ		exp	
	$\Delta G^{\ddagger}$	K	$\Delta G^{\ddagger}$	k	$\Delta G^{\ddagger}$	k	k_{exp}	ref
110	44.51	1.45×10^{-20}	38.96	1.64×10^{-16}	36.75	6.86×10^{-15}		
111	24.70	4.85×10^{-6}	19.82	1.79×10^{-2}	20.38	6.95×10^{-3}	$3.4 \pm 0.2 \times 10^{-3}$, 1.6×10^{-3}	5, 6
210	37.62	1.64×10^{-15}	33.90	8.44×10^{-13}	32.42	1.02×10^{-11}		
211	22.79	1.22×10^{-4}	17.87	4.85×10^{-1}	19.12	5.84×10^{-2}	$5.5 \pm 0.3 \times 10^{-3}$	6
220	41.05	5.00×10^{-18}	32.61	7.38×10^{-12}	33.34	2.15×10^{-12}		
221	29.13	2.74×10^{-9}	21.06	2.21×10^{-3}	22.48	2.0×10^{-4}	$<1.2 \times 10^{-4}$	21

proceed in the gas phase. However, incorporation of one water molecule into the reaction would dramatically catalyze the reaction. As seen from Table 1 and Figure 6a, both activation enthalpy and activation Gibbs free energy for the reaction of $(RC)_{111} \rightarrow (TS)_{111} \rightarrow (PC)_{111}$ are decreased by about half of those in gas phase. The rate constant is increased by 15 orders while the half-life time is shortened by 15 orders of magnitude. The significant water catalytic effect could be accounted for by formation of the strong hydrogen bond between the CH_2-Cl(OH) hydrogen (OH) and water oxygen and the strong stabilization of leaving Cl atom by an interaction of $H_3O^+Cl^-$ pairs for the transition structure. Another possible reason is that the NPA charge redistribution from $(RC)_{111}$ to $(TS)_{111}$ is smaller by 0.15e as compared to that in the gas phase i.e., from $(RC)_{110}$ to $(TS)_{110}$. The presence of water in the reaction system appears to significantly stabilize the TS relative to that of the reactants, where the localization of charge is not as acute as mentioned before. Incorporation of two water molecules reduces the activation enthalpy and activation Gibbs free energy by another 4.9 and 3.6 kcal/mol, respectively. Both the rate constant and the half-life time are changed by another 5 orders of magnitude. A third water molecule (from $n = 2$ to 3) decreases $\Delta H^{\ddagger}_{11n}$ by an additional 3.7 kcal/mol and $\Delta G^{\ddagger}_{11n}$ by an additional 5.0 kcal/mol. However, the fourth water molecule (from $n = 3$ to 4) has only a modest additional catalytic effect in which $\Delta H^{\ddagger}$ and $\Delta G^{\ddagger}$ are decreased by only 2.6 and 0.8 kcal/mol, respectively.

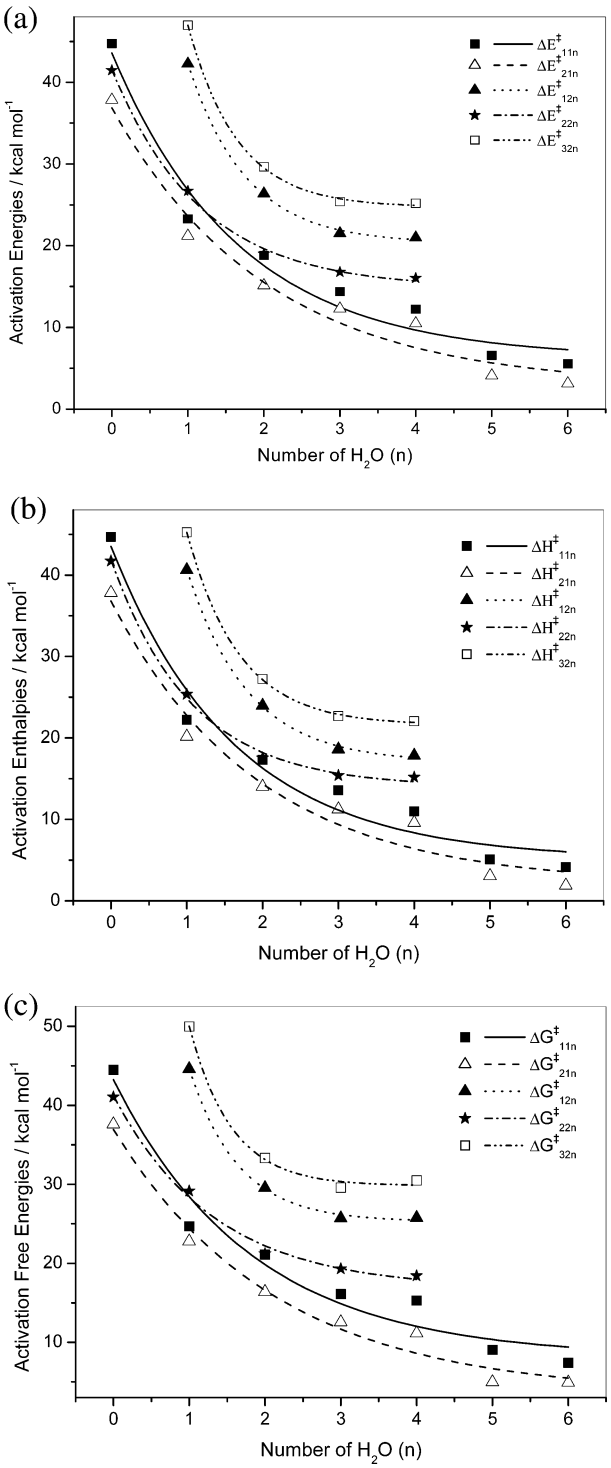

Figure 7. Plot of the barriers to reaction (in kcal/mol) from the RC to the TS for the $CH_2(OH)Cl + nH_2O \rightarrow HCHO + nH_2O + HCl$ ($n = 0$, 1, 2, ..., 6) (e.g., solid squares for ΔE_{11n}); $HCHO + nH_2O \rightarrow CH_2(OH)_2 + (n-1)H_2O$ ($n = 1$, 2, ..., 4) (e.g., solid triangles for ΔE_{12n}); $CH(OH)Cl_2 + nH_2O \rightarrow ClCHO + nH_2O + HCl$ ($n = 0$, 1, 2, ..., 6) (e.g., open triangles for ΔE_{21n}); $ClCHO + nH_2O \rightarrow CO + HCl + nH_2O$ ($n = 0$, 1, 2, ..., 4) (e.g., + for ΔE_{22n}); and $ClCHO + nH_2O \rightarrow CH(Cl)(OH)_2 + (n-1)H_2O$ ($n = 1$, 2, ..., 4) (e.g., open squares for ΔE_{32n}) reactions as a function of the number of H_2O molecules. The lines give a best-fit exponential function to the barrier heights to the reactions as a function of the number of H_2O molecules.

As more water molecules $n = 5$ are added to the reaction, $\Delta H^{\ddagger}_{11n}$ and $\Delta G^{\ddagger}_{11n}$ are significantly decreased by another 5.9 and 6.3 kcal/mol, respectively. However, the sixth water molecule (from $n = 5$ to 6) has only a modest additional catalytic effect in which $\Delta H^{\ddagger}_{11n}$ and $\Delta G^{\ddagger}_{11n}$ are decreased by only 0.9 and 1.6 kcal/mol, respectively. This is similar to the case from $n = 3$ to 4. It appears the activation energies ($\Delta E^{\ddagger}_{11n}$), barriers ($\Delta H^{\ddagger}_{11n}$), and Gibbs free energy ($\Delta G^{\ddagger}_{11n}$) can be reasonably described as an exponential decay process as the number of water goes from $n = 0$ to $n = 6$ as shown in Figure 7. Note that it is unexpected that $\Delta H^{\ddagger}_{11n}$ and $\Delta G^{\ddagger}_{11n}$ for $n = 3$ and 4 are noticeably larger than those of the other water catalytic reactions. This may be rationalized by the existence of the strong hydrogen bonds between $CH_2Cl(OH)$ hydrogen (OH) and the water oxygen (O4 or O5) in $(RC)_{113}$ and $(RC)_{114}$ while no equivalent hydrogen bonds are formed for the other water-based RC. The existence of these hydrogen bonds for O1- - -O4 and

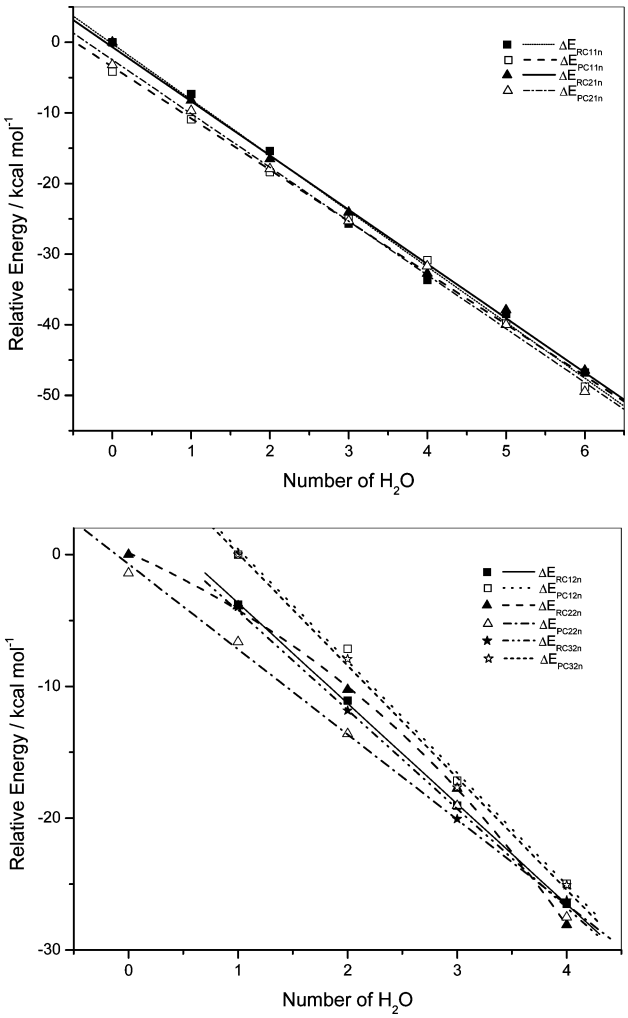

Figure 8. (a) Plot of the stabilization energy (in kcal/mol) of the RC and PC for the $CH_2(OH)Cl + nH_2O \rightarrow HCHO + nH_2O + HCl$ ($n = 0$, 1, 2, ..., 6) (e.g., solid squares for ΔE_{RC11n} and open squares for ΔE_{PC11n}) and $CH(OH)Cl_2 + nH_2O \rightarrow ClCHO + nH_2O + HCl$ ($n = 0$, 1, 2, ..., 6) (e.g., closed triangles for ΔE_{RC21n} and open squares for ΔE_{PC21n}) reactions as a function of the number of H_2O molecules. The lines give best-fit linear function to the stabilization energies for the RC and PC as a function of the number of H_2O molecules. (b) Plot of the stabilization energy (in kcal/mol) of the RC and PC for the $HCHO + nH_2O \rightarrow CH_2(OH)_2 + (n-1)H_2O$ ($n = 1$, 2, ..., 4) (e.g., solid squares for ΔE_{RC12n} and open squares for ΔE_{PC12n}); $ClCHO + nH_2O \rightarrow CO + HCl + nH_2O$ ($n = 0$, 1, 2, ..., 4) (e.g., closed triangles for ΔE_{RC22n} and open squares for ΔE_{PC22n}); and $ClCHO + nH_2O \rightarrow CH(Cl)(OH)_2 + (n-1)H_2O$ ($n = 1$, 2, ..., 4) (e.g., closed stars for ΔE_{RC32n} and open stars for ΔE_{PC32n}) reactions as a function of the number of H_2O molecules. The lines give best-fit linear function to the stabilization energies for the RC and PC as a function of the number of H_2O molecules.

O1- - -O5 in $(RC)_{113}$ and $(RC)_{114}$ can significantly stabilize the RC structure and deactivate the C−Cl bond [the C−Cl bonds in $(RC)_{113}$ and $(RC)_{114}$ are only slightly elongated as compared to those in the gas phase] more than other hydrogen-bonded RC, therefore resulting in larger $\Delta H^{\ddagger}_{11n}$ and $\Delta G^{\ddagger}_{11n}$.

We note that both the RCs and the PCs are significantly stabilized by the interaction of the reactant $CH_2Cl(OH)$ molecule or the product molecules HCHO and HCl with the H_2O molecules via hydrogen bondlike interactions as discussed in the preceding subsections. The stabilization energies of the $[CH_2Cl(OH)](H_2O)_n$ cluster or $(RC)_{11n}$ relative to the separated reactants $[CH_2Cl(OH) + nH_2O]$ are found to be 0.0, −7.3, −15.4, −25.7, −33.7, −38.5, and −46.8 kcal/mol for $n = 0-6$, respectively. The 7.3 kcal/mol of interaction energy between $CH_2Cl(OH)$ and H_2O suggests a more stable complex than that found for water dimers, indicating a stronger hydrogen bond than that in water dimers. The interaction energy becomes more negative as further water molecules are incorporated; this is a result of the increased strength of the interaction and number of hydrogen bonds formed. The stabilizing effect increases fairly steadily with only a slightly larger stabilization occurring for $n = 3$ and 4. As shown in Figure 8a, the stabilization energies ΔE_{RC11n} possess a linear relationship with the number of water molecules (n); i.e., ΔE_{RC11n} (kcal/mol) $\approx -0.229-7.888n$, where n is the number of water molecules in the water-solvated reactant clusters. The stabilization energy ΔE_{RC11n} of the PC $[(HCHO)(HCl)(H_2O)_n]$ or $(PC)_{11n}$ relative to the separated products $(HCHO + HCl + nH_2O)$ are computed to be −4.1, −10.9, −18.4, −20.3, −30.8, −39.9, and −48.8 kcal/mol for $n = 0-6$, respectively (Table 1). The behaviors of these PCs clusters are quite similar to those of RCs and the $HCl(H_2O)_n$ clusters. It is interesting to compare these results to those previously found for the dissolution of strong acids (HCl) by H_2O molecules.[35−38] It was found experimentally[37] that in argon-matrix studies a cluster with an HCl to H_2O ratio of 1:3 is not yet ionic, whereas from 1:4 onward the cluster is best described as $Cl^--(H_2O)_n-H_3O^+$ ($n > 3$). Several recent calculations[38] have confirmed this experimental result. The interaction energies for the most stable isomer of $(HCl)(H_2O)_n$ clusters were found to be −4.1, −10.2, −19.2, −24.5, and −36.1 kcal/mol for $n = 1-5$, respectively.[35] The stabilization energies for $(HCl)(H_2O)_n$ clusters as $n = 1$, 2, 3 are quite close to those of $(PC)_{11n}$ where $n = 0$, 1, 2 if the HCHO can be regarded as a H_2O molecule in the $(PC)_{11n}$. However, the stabilization energies of $(PC)_{11n}$ for $n = 3$ and 4 are smaller by about 4.0 kcal/mol as compared to those of $(HCl)(H_2O)_n$ where $n = 4$ and 5. It is noted that the $(HCl)(H_2O)_n$ clusters prefer a nondissociated structure when $n = 1-3$ while the structure with $n = 4$ and 5 prefers dissociated structures.[35,36] This is consistent with the fact that the PC $[(HCHO)(HCl)(H_2O)_n]$ or $(PC)_{11n}$ prefers nondissociated structures with $n = 1-3$ and prefer dissociated structures with $n = 4$, 5, and 6. The behaviors of the PCs are also consistent with the solvation shell, for the reaction becomes built up through three major processes mentioned earlier: the 2D solvation shell for $n = 1$ and 2, the transition from 2D to 3D for $n = 3$ and 4, and the 3D full solvation shell for $n = 5$ and 6.

It is instructive to compare our computed thermodynamic data to those for the experimental gas phase decomposition reactions of $CH_2Cl(OH)$ into HCl + HCHO.[5,6] The experimental rate constant of the reaction ranges from 1.6×10^{-3} to 3.4×10^{-3} s^{-1} depending on the different chamber used in the experiments, resulting in measured lifetimes ranging from 204 to 433 s.[6] However, the computed gas phase reaction rate constant is only 1.0×10^{-20} s^{-1}; the half-life time is as long as 6.8×10^{19} s, and this corresponds to an order of 10^{12} years for room temperature unimolecular decomposition! It is very difficult to explain why the reaction occurs in gas phase for such a long theoretical calculated half-life time. The much shorter measured lifetime and the probable wall effect suggest that traces of water could play an important role in its decomposition. It is interesting that the calculated rate constant of 2×10^{-3} s^{-1} at the MP2/6-31+G** level for the two-water catalytic reaction shown in Table 1 is comparable to the measured rate constants. The calculated rate constants are 1.79×10^{-2} and 6.95×10^{-3} s^{-1} at the MP2/aug-cc-pVDZ and QCISD(T)/aug-cc-pVDZ levels of theory, respectively, for the one-water catalytic reaction. Therefore, we speculate that traces of water in the chamber may be the most possible catalyst of the decomposition reaction. The one- or two-water-involved cyclic catalytic reaction could be the most possible reaction pathway for the gas phase decomposition reaction. Different amounts of water on the walls of the different size reaction chambers could affect the reaction rate and decay time as shown in Table 1 and Figure 6 and can possibly explain why the measured experimental rate constants and lifetimes are different in different sizes of reaction vessels.[5,6] As more water molecules become involved in the reaction, we expect that the decomposition reactions would become faster. On the basis of the trends in the activation enthalpies and activation free energies, it can be concluded that, if sufficient water is available or the water concentration is increased, the decomposition reaction can proceed via a cooperative mechanism in the gas phase and also in aqueous solution. In the gas phase, this mechanism involves active catalysis by one or two water molecules while in the water solution phase, and this mechanism involves active catalysis by five or six (or more) water molecules. The three- and four-water catalytic reaction mechanism can be regarded as a mechanism that the water only partially solvates the reaction system or something between the gas phase and the water solution. Therefore, we predict that the decomposition reaction can be much faster (the rate constant would be in the order of 10^5 to 10^9 s^{-1} in aqueous solution) and can even proceed by a hydration reaction with the decomposition product HCHO to produce methanediol $[CH_2(OH)_2]$. We shall discuss this reaction in the next subsection.

2. $HCHO + nH_2O \rightarrow CH_2(OH)_2 + (n-1)H_2O$ (Where $n = 1, 2, 3, 4$). It has been experimentally shown that formaldehyde (HCHO) in aqueous solution undergoes water addition to produce methanediol $[CH_2(OH)_2]$.[39−41] It is interesting to note that a theoretical investigation of this reaction at the level of MP2/6-31G* indicates that this reaction may proceed mainly through a cooperative mechanism with three H_2O molecules hydrating the carbonyl group.[42] This cooperative mechanism is similar to the water-catalyzed $CH_2Cl(OH)$ HCl elimination reaction that we studied in the preceding subsection. Our recent experiments have shown that observed ultraviolet photolysis of low concentrations of CH_2I_2 in water leads to almost complete conversion into $CH_2(OH)_2$ and 2HI products.[43] Ab initio computational results indicate that the CH_2I-I species generated by the photolysis of CH_2I_2 can react readily with water via a water-catalyzed O−H insertion/HI elimination reaction to produce $CH_2I(OH)$ + HI followed by the $CH_2I(OH)$ product and then undergoes a further water-catalyzed HI elimination reaction to form $H_2C{=}O$ + HI. The $H_2C{=}O$ product further reacts with water to form the other final $CH_2(OH)_2$ product seen in the photochemistry experiments.[53]

Inspection of Figure 2 shows that a cyclic reaction mechanism containing 1−4 water molecules is found from the MP2/6-

31+G** calculations. This mechanism is quite similar to the cyclic (cooperative) proposed by Eigen and Wolfe.[42] The calculated cyclic geometries of RCs, TSs, and PCs shown in Figure 2 are also consistent with those proposed by Eigen and Wolfe.[42] The $\Delta E^{\ddagger}$, $\Delta H^{\ddagger}$, and $\Delta G^{\ddagger}$ with $n = 1-2$ are quite close to those in ref 43. Our calculated activation parameters $\Delta E^{\ddagger}$, $\Delta H^{\ddagger}$, and $\Delta G^{\ddagger}$ at a larger basis set 6-31+G** with diffuse functions predict some saturation of the catalytic effect as three and four water molecules are involved in the reaction. However, previous calculations[42] showed that the third water molecule (from $n = 3$ to 4) has an inhibitory effect that gave slightly larger $\Delta E^{\ddagger}$, $\Delta H^{\ddagger}$, and $\Delta G^{\ddagger}$ values for $n = 3$ than the values for $n = 4$. This may be due to the smaller basis set effect used since no p polarization for hydrogen atoms and no diffuse functions were considered in the previous calculations.[42] Overall, our present results are in good agreement with the previous work of Eigen and Wolfe.[42] We note that there exists a good exponential decay relationship of the values for $\Delta E^{\ddagger}_{12n}$, $\Delta H^{\ddagger}_{12n}$, and $\Delta G^{\ddagger}_{12n}$ as a function of the number of water molecules (see Figure 7a−c). This indicates that a saturation effect will almost be reached as four water molecules are incorporated into the reaction. The stabilization energy of the RCs and PCs relative to the separated reactants or products is computed and listed in Table 1. There exists a good linear relationship of the stabilization energies with the number of water as shown in Figure 8b. We think that as four water molecules are incorporated into the reaction system, a mostly formed solvation shell could be established.

B. Decomposition of Dichloromethanol in Gas Phase and in Aqueous Solution into CO + HCl. *1. $CH(OH)Cl_2 + nH_2O \rightarrow ClCHO + HCl + nH_2O$ (Where n = 0, 1, 2, 3, 4, 5, 6).* Figure 3 displays the optimized geometry found for the reactions of $CHCl_2(OH) + nH_2O \rightarrow ClCHO + HCl + nH_2O$, i.e., $(RC)_{21n} \rightarrow (TS)_{21n} \rightarrow (PC)_{21n}$ where $n = 0, 1, 2, 3, 4, 5, 6$. Analogous to the gas phase decomposition reaction of $CH_2Cl(OH) \rightarrow HCl + HCHO$, the gas phase decomposition reaction of $CHCl_2(OH) \rightarrow HCl + ClCHO$ undergoes a similar four-centered cyclic TS $(TS)_{210}$ to produce the HCl and ClCHO products. The structures for the RC, TS, and PC are quite similar to those of $CH_2Cl(OH)$ gas phase decomposition reaction. In the one- and two-water catalytic reactions, the RCs, TSs, and PCs are structurally similar to the corresponding ones found in the decomposition of $CH_2Cl(OH)$. However, in the three-water catalytic reaction, the $(RC)_{213}$ has a different conformation from the corresponding $(RC)_{113}$. In the four-, five-, and six-water catalytic reactions, the structural features for most of the $(RC)_{21n}$ and $(TS)_{21n}$ where $n = 4, 5, 6$ are very similar to those of the analogous $(RC)_{11n}$ and $(TS)_{11n}$ where $n = 4, 5, 6$. The main difference is that each of the formyl chloride (ClCHO) in the PC $(PC)_{21n}$ ($n = 4, 5, 6$) was rotated by about 90° and a new H···Cl interaction was formed between the ClCHO hydrogen atom and the leaving Cl atom while in the other PCs, the leaving Cl atoms have weak interactions with the carbon atoms of the products HCHO or ClCHO as shown in Figures 1 and 3.

Examination of Table 1 and Figure 6b shows that the gas phase decomposition reaction of $CHCl_2(OH) \rightarrow HCl + ClCHO$ has an activation barrier of 37.8 kcal/mol and is exothermic by about 5.6 kcal/mol. This predicted exothermicity of the decomposition reaction for dichloromethanol is slightly larger than the calculated $\Delta H(298.15)$ of 2.5 kcal/mol obtained from MP2/6-311G(2d,p) calculations.[5] However, our calculated value is consistent with the experimental estimation of 8.8 kcal/mol.[5] The activation Gibbs free energy and Gibbs free energy are computed to be 37.6 and −9.8 kcal/mol, respectively, giving a rate constant of 1.6×10^{-15} and a half-life time of 4.2×10^{14} s. The rate constant is larger by 5 orders of magnitude, and the lifetime is shortened by 5 orders of magnitude since both the activation barrier and the free energy are smaller by 6.9 kcal/mol as compared to the analogous reaction of $CH_2Cl(OH) \rightarrow HCl + HCHO$. Another different feature is that the reaction of $CHCl_2(OH) \rightarrow HCl + ClCHO$ is exothermic while the analogue reaction of $CH_2Cl(OH) \rightarrow HCl + HCHO$ is slightly endothermic. These activation and kinetics parameters imply that the decomposition reaction of $CHCl_2(OH) \rightarrow HCl + ClCHO$ is faster than that of $CH_2Cl(OH) \rightarrow HCl + HCHO$. This is qualitatively consistent with the experimental observations that the former reaction had a slightly smaller reaction constant than that of the later reaction.[5,6] However, the predicted activation barrier of 37.6 kcal/mol is still too big to compare to the experimental rate constant of $\sim 10^{-3}$ s^{-1}.[5,6] As expected, water molecules can catalyze these reactions. Incorporation of 1−6 water molecules into the reactant $CH_2Cl(OH)$ can noticeably accelerate the decomposition reaction. As demonstrated in Figure 6b, the activation energies are predicted to be 37.8, 21.2, 15.1, 12.3, 10.5, 4.1, and 3.1 kcal/mol with $n = 0-6$, respectively. It is interesting to note that the activation energies are systematically smaller than those with the same number of water molecules for reaction 1, indicating that the former reaction is faster than the latter. The main features for $\Delta H^{\ddagger}$ and $\Delta G^{\ddagger}$ for reaction 2 are quite similar to those of reaction 1. Similarly, the activation energies ($\Delta E^{\ddagger}_{21n}$), barriers ($\Delta H^{\ddagger}_{21n}$), and Gibbs free energy ($\Delta G^{\ddagger}_{21n}$) for reaction 2 can be reasonably described as an exponential decay as the number of water goes from $n = 0$ to $n = 6$ as shown in Figure 7. Note that it is unexpected that $\Delta H^{\ddagger}_{21n}$ and $\Delta G^{\ddagger}_{21n}$ for $n = 4$ are noticeably larger than those of the other water catalytic reactions. This can possibly be explained by the existence of the strong hydrogen bonds between the $CHCl_2(OH)$ hydrogen (OH) and the water oxygen (O5) in the $(RC)_{214}$ while no equivalent hydrogen bonds are formed for the other water-based RCs. The existence of the hydrogen bonds for O1- - -O5 in $(RC)_{214}$ can significantly stabilize the $(RC)_{214}$ structure and result in larger $\Delta E^{\ddagger}_{214}$, $\Delta H^{\ddagger}_{214}$, and $\Delta G^{\ddagger}_{214}$ and ΔE_{214}, ΔH_{214}, and ΔG_{214}.

Although qualitatively reaction 2-1 with the same number of water molecules is faster than reaction 1-1 and this is consistent with the experimental observations, it is still hard to compare the predicted activation data with those experimental data. As mentioned above, water molecules can noticeably reduce the reaction barrier and accelerate the reaction. As shown in Table 1, the one-water catalytic reaction has a slighter smaller rate constant ($\sim 1.2 \times 10^{-4}$ s^{-1}) than the experimental observations measured as $(k = 5.5 \pm 0.3) \times 10^{-3}$ s^{-1} for reaction 2-1 in gas phase[5,6] while the two-water catalytic reaction has a larger rate constant ($\sim 6.1 \times 10^{0}$ s^{-1}). The calculated rate constants are 4.85×10^{-1} and 5.84×10^{-2} s^{-1} at the MP2/aug-cc-pVDZ and QCISD(T)/aug-cc-pVDZ levels of theory, respectively, for the one-water catalytic reaction. Therefore, the gas phase reaction of 2-1 can probably be reasonably modeled as one- or two-water molecule-involved reactions and this is consistent with the experimental observations.

We note that a recent experimental decomposition reaction of 2-1 in aqueous solution[19] makes it possible for us to make a direct comparison between experiment and theory for this reaction. This study estimated that the decomposition of $CHCl_2(OH)$ took place with $t_{1/2} < 20$ μs in aqueous solution,[19] which corresponds to a lower limit for the rate constant of 3.5×10^{4} s^{-1}. It can be seen from Table 1 that the decomposition of

$CHCl_2(OH)$ with four water molecules was estimated to be 4.2×10^4 s^{-1}, in excellent agreement with the experimental observed rate constant in aqueous solution. However, it should be noted that the experimental measured rate constant was only a lower limit from an approximate estimation. The cubic or cubiclike model reaction with five or six water molecules was computed to have a much larger rate constant on the order of $\sim 10^9$ s^{-1}. Considering the decomposition of ClCHO into CO + HCl had a rate constant $k = 10^4$ s^{-1} and the lower limit ($k > 4.2 \times 10^4$ s^{-1}) for the reaction of 2-1 measured in aqueous solution,[19] we believe that the decomposition of $CHCl_2(OH)$ into ClCHO + HCl in aqueous solution would take place even faster than the subsequent decomposition reaction of ClCHO into CO + HCl and most probably the decomposition of $CHCl_2$-(OH) could have a larger rate constant of about 10^5-10^9 s^{-1} in aqueous solution. The subsequent decomposition reaction of ClCHO into CO + HCl may be the rate-determining step for the overall reaction 2. We shall discuss the decomposition reaction of ClCHO in detail in the following subsection.

Similar to the stabilization energies ΔE_{RC11n} of chloromethanol, the stabilization energies ΔE_{RC21n} where $n = 0, 1, ..., 6$ relative to the separated reactants of dichloromethanol and water molecules possess a similar relationship with the number of water molecules with a relation of ΔE_{RC11n} (kcal/mol) $\approx -0.677-7.680n$, where n is the number of water molecules in the water-solvated reactant clusters as shown in Figure 8a. It appears that each water molecule contributes approximately about 7.7 kcal/mol to the RC clusters for both reactions 1-1 and 2-1. The stabilization energies ΔE_{PC21n} of PC relative to the separated products of ClCHO + HCl + $n$$H_2O$ have a similar relationship with the number of water molecules (n) as shown in Figure 8a. The stabilization energies of ΔE_{RC11n}, ΔE_{PC11n}, ΔE_{RC21n}, and ΔE_{PC21n} for reactions 1-1 and 2-1 are very similar for the same number of water molecules as shown in the Figure 8a, indicating a similar solvation trend for both reactant water clusters and product water clusters. Examination of the reaction enthalpies in Table 2 shows that the exothermic properties for reaction 2-1 are very close for the different number of water-solvated reactions. The endothermic properties for reaction 1-1 have a similar trend except that the ΔH with $n = 3$ and 4 has noticeably larger values as compared to the other water-solvated reactions.

2. $ClCHO + nH_2O \rightarrow CO + HCl + nH_2O$ (Where $n = 1, 2, 3, 4$). Decomposition of formyl chloride into HCl and CO in the gas phase and in aqueous solution can be modeled as shown in Figure 4, namely, ClCHO + $n$$H_2O$ → CO + HCl + $n$$H_2O$ or $(RC)_{22n} \rightarrow (TS)_{22n} \rightarrow (PC)_{22n}$ where $n = 0, 1, 2, 3, 4$. The structural features of the RCs, TSs, and PCs are quite similar to those of mono- and dichloromethanols. It is shown that the two-water catalytic reactant cluster can be regarded as a weakly bonded water cluster between the water dimer and the ClCHO molecule. The three-water catalytic reaction can be regarded as the formation of a $(RC)_{223}$ by insertion of HClCO molecule into water trimer $(H_2O)_3$. Similar to the cases of chloromethanol and dichloromethanol, the H···Cl interactions in $(RC)_{221}$ and $(RC)_{222}$ become systematically shortened (from 2.581 to 2.452 Å). However, the geometry of $(RC)_{224}$ is somewhat different from the proceeding water-solvated RCs, in which a hydrogen bond between one of the O2 atom of a cyclic water tetramer $(H_2O)_4$ and H atom of ClCHO molecule while the leaving Cl atom almost has no interactions with hydrogen atoms in the water tetramer. It should be noted that in $(RC)_{224}$ the geometry of the cyclic water tetramer $(H_2O)_4$ is only slightly perturbed by the interaction of the ClCHO hydrogen atom with the water tetramer. Most of the TS structures are similar to those found for the chloromethanol and dichloromethanol decomposition reactions. The one and two catalytic TS structures are cycliclike hydrogen-bonded conformations, in which the leaving Cl atoms are stabilized by the nearby water hydrogen atom. However, for the three- and four-water catalytic TS structures, the leaving Cl atoms are stabilized by two hydrogen atoms in the nearby water molecules. It is interesting to note that $(TS)_{223}$ and $(TS)_{224}$ have booklike geometries. This implies that a structural rearrangement will occur in going from $(RC)_{224}$ to $(TS)_{224}$ as shown in Figure 4 in that both the transition structures and the PC require two H···Cl interactions.

It is shown in Table 1 that the activation free energy and reaction barrier in the gas phase for the decomposition of ClCHO into HCl and CO are predicted to be 41.05 and 41.46 kcal/mol at the MP2/6-31+G(d,p) level of theory. The reaction is exothermic by 6.86 kcal/mol at the same level of theory. The rate constant is predicted to be on the order of 10^{-18} s^{-1}. The activation free energies become 32.61 and 33.34 kcal/mol for MP2/aug-cc-pVDZ and QCISD(T)/aug-cc-pVDZ levels of theory, respectively, as shown in Table 2. Our calculation results are consistent with the 43.95 kcal/mol of calculated dissociation barrier to HCl + CO by Tyrrell and co-workers[22] at the MP2 level of theory and the 41.1 kcal/mol at the PMP4SDTQ level of theory by Francisco.[44] Our predicted heat of reaction is also consistent with the value of −5.9 reported by Francisco.[44]

The decomposition of formyl chloride into CO + HCl products was measured in the gas phase, and the lifetime of HClCO was estimated to be 10 min in a 0.1 dm^3 reaction container[20] and between 28 and 190 min in a 480 dm^3 reaction container.[21] The first-order rate constant for the loss of ClCHO at the walls was determined to be in the range of 6×10^{-5} to 4×10^{-4} s^{-1}.[21] The second-order rate constant of the reaction of ClCHO with water vapor was predicted to be less than 5×10^{22} cm^3/s.[21] If the water concentration of 2.5×10^{17} cm^{-3} was used, the first-order rate constant for the decomposition of ClCHO is calculated to be less than 1.2×10^{-4} s^{-1}. However, the calculated rate constants for the decomposition of ClCHO from the literature[21] and our own calculations at the MP2/6-31+G** level of theory for the decomposition of formyl chloride into CO + HCl are all far away from the experimental values. Note that the measured lower bound first-order rate constant of the reaction ClCHO with water vapor is in the range of the rate constants reported previously for gas phase decomposition of ClCHO. This and probable wall effects suggest that the traces of water on the reaction walls could play an important role in the gas phase decomposition of ClCHO. As expected, the activation free energy is decreased from 41.05 kcal/mol for the gas phase decomposition to 29.13 kcal/mol for the one-water-involved reaction at the MP2/6-31+G** level of theory as shown in Table 2. The activation free energies are predicted to be 21.06 and 22.48 kcal/mol for MP2/aug-cc-pVDZ and QCISD(T)/aug-cc-pVDZ levels of theory, respectively. The corresponding rate constants for the loss of ClCHO are predicted to be 2.21×10^{-3} and 2.0×10^{-4} s^{-1}, respectively. This is in good agreement with the gas phase experimental observations. It appears that water can dramatically catalyze the decomposition reaction of ClCHO.

By adding water molecules one by one to the RC, the decomposition reaction will be further catalyzed as shown Table 1 and Figure 6b. Similar to the cases of chloromethanol and dichloromethanol, the activation energies ($\Delta E^{\ddagger}_{22n}$), activation enthalpies ($\Delta H^{\ddagger}_{22n}$), and activation Gibbs free energy ($\Delta G^{\ddagger}_{22n}$) for reaction 2-2 can be described by an exponential decay

TABLE 3: MP2/aug-cc-pVDZ//MP2/6-31+G Calculated Activation Free Energies ($\Delta G^{\ddagger}_{gas}$, kcal mol^{-1}), Rate Constant (k_{gas}, s^{-1}), and Stabilization Free Energies of RC [$\Delta G_{RC}{}^{N}$ (No BSSE Correction), $\Delta G_{RC}{}^{B}$ (BSSE Corrected), and $\Delta G_{RC}{}^{G3MP2}$)[a] (kcal mol^{-1})] Relative to Separated Reactants and Products in Gas Phase and the Activation Free Energies ($\Delta G^{\ddagger}_{solv}$,[b] kcal mol^{-1}) and Rate Constant (k_{solv}, s^{-1}) in Aqueous Solutions**

	gas phase model					D-PCM model	
reaction	$\Delta G_{RC}{}^{N}$	$\Delta G_{RC}{}^{B}$	$\Delta G_{RC}{}^{G3MP2}$	$\Delta G^{\ddagger}_{gas}$	k_{gas}	$\Delta G^{\ddagger}_{solv}$	k_{solv}
1-1: $CH_2(OH)Cl + nH_2O \rightarrow HCHO + nH_2O + HCl$ ($n = 0, 1, 2, ..., 6$)							
110				38.96	1.64×10^{-16}	32.03	1.97×10^{-11}
111	0.89	2.35	1.02	19.82	1.79×10^{-2}	15.57	2.33×10^{1}
112	1.45	4.25	1.98	17.33	1.20×10^{0}	11.82	1.33×10^{4}
113	2.44	7.63	2.83	10.55	1.14×10^{5}	9.05	1.44×10^{6}
114	3.45	9.95	2.87	9.72	4.56×10^{5}	9.01	1.53×10^{6}
115	5.65	14.23	6.74	6.52	1.03×10^{8}	6.84	5.92×10^{7}
116	9.15	20.06	9.12	5.15	1.03×10^{9}	5.77	3.63×10^{8}
2-1: $CH(OH)Cl_2 + nH_2O \rightarrow ClCHO + nH_2O + HCl$ ($n = 0, 1, 2, ..., 6$)							
210				33.90	8.44×10^{-13}	27.38	5.13×10^{-8}
211	−0.11	1.54	0.26	17.87	4.85×10^{-1}	14.73	9.70×10^{1}
212	1.26	4.85	1.15	13.05	1.64×10^{3}	8.10	7.12×10^{6}
213	2.38	7.52	1.87	8.58	3.15×10^{6}	7.00	4.52×10^{7}
214	5.00	12.63	3.53	6.56	9.52×10^{7}	5.54	5.39×10^{8}
215	7.62	16.92	7.92	3.13	3.16×10^{10}	4.48	3.21×10^{9}
216	10.03	21.70	10.03	3.22	2.71×10^{10}	5.13	1.08×10^{9}
2-2: $ClCHO + nH_2O \rightarrow CO + HCl + nH_2O$ ($n = 0, 1, 2, ..., 4$)							
220				32.61	7.38×10^{-12}	27.17	7.25×10^{-6}
221	2.94	3.87	3.24	21.06	2.21×10^{-3}	16.96	2.24×10^{0}
222	5.29	7.84	5.02	15.01	6.03×10^{1}	11.39	2.75×10^{4}
223	7.08	11.01	6.20	13.35	9.96×10^{2}	11.61	1.89×10^{4}
224	7.24	13.06	6.90	11.81	1.34×10^{4}	11.76	1.47×10^{4}

[a] $\Delta G_{RC}{}^{G3MP2}$: Stabilization free energy from G3MP2 calculations. [b] $\Delta G^{\ddagger}_{solv} = \Delta G^{\ddagger}_{gas} + \Delta\Delta G^{\ddagger}_{solv}$, where $\Delta G^{\ddagger}_{gas}$ is the activation free energy at the theory of MP2/aug-cc-pVDZ level and $\Delta\Delta G^{\ddagger}_{solv}$ is defined as the difference between the solvation energy of RC and the TS from B3LYP/Aug-cc-pVDZ calculations. MP2/aug-cc-pVDZ-DPCM-BONDI calculations obtained very similar activation free energies (30.39, 15.73, 10.51, 10.47, and 12.03 kcal/mol for $n = 0$, 1, 2, 3, and 4) in aqueous solutions for reaction 2-2. The stabilization free energies for $(RC)_{221-4}$ were calculated to be 3.11, 4.48, 5.16, and 5.04 kcal/mol, respectively, at the G3 level.

process as the number of waters goes from $n = 0$ to $n = 4$ (see Figure 7). This indicates that a smaller number of water molecules, probably equal to or less than four water molecules, may be needed to build the first solvation shell for the decomposition reaction of ClCHO in aqueous solution as compared to those of $CH_2Cl(OH)$ and $CHCl_2(OH)$, in which five or six molecules were used to build a solvation shell. We speculate that the difference for usage of water molecules in building the solvation clusters could be due to the different hybridization of the carbon atom for $CH_2Cl(OH)$ and $CHCl_2$-(OH) as compared to ClCHO because in ClCHO the carbon atom has a sp^2 hybrid that need less water molecules for building the solvation shell, whereas both $CH_2Cl(OH)$ and $CHCl_2(OH)$ carbon atoms have sp^3 hybrids that need more water for building solvation shells. A similar behavior was found for the stabilization energies relative to separated products and also occur for the PC as shown in Figure 8.

Although some saturation effects appear to occur when four explicit water molecules were included in the reaction model from the $\Delta E^{\ddagger}_{22n}$, $\Delta H^{\ddagger}_{22n}$, and $\Delta G^{\ddagger}_{22n}$ shown in Figures 6 and 7, the calculated rate constant of 2×10^{-1} s^{-1} from the MP2/6-31+G** level of theory is still far different as compared to those experimentally observed pseudo-first-order rate constant 1×10^{4} s^{-1}.[19] However, at the MP2/aug-cc-pVDZ level of theory, the predicted rate constant of 1.3×10^{4} s^{-1} for the four-water catalytic reaction is in good agreement with the experiment observations in aqueous solution as shown in Table 3.

It appears that the larger aug-cc-pVDZ basis set with both polarization and diffuse functions included for both light and heavy atoms predicts more stable transition structures with the zwitterionic $(H_2O)_nH_3O^+Cl^-$ species more than the neutral reactant clusters as compared to the smaller 6-31+G** basis set. This is reasonable since the larger aug-cc-pVDZ basis set may provide a better description of charge distributions for the zwitterions $(H_2O)_nH_3O^+Cl^-$ form in the TS. The overall improvement in predicting the rate constants by the aug-cc-pVDZ basis set for both gas phase and solution phase for all reactions 1-1, 2-1, and 2-2 indicates that it is probably necessary to use a basis set including both polarization and diffuse functions for light and heavy atoms in order to obtain a better description of charge distributions for the charge-separated species found in these HCl elimination reactions.

C. Decomposition of Dichloromethanol in Aqueous Solution to Produce HCOOH Product: Reactions of ClCHO + $nH_2O \rightarrow CHCl(OH)_2 + (n-1)H_2O$ (Where $n = 1, 2, 3, 4$) and $CHCl(OH)_2 + nH_2O \rightarrow HCOOH + nH_2O$ (Where $n = 0, 1$). In addition to the decomposition reaction of $CHCl_2(OH)$ to produce formyl chloride (ClCHO) and hydrogen chloride (HCl) (2-1) in aqueous solution followed by decomposition of formyl chloride into CO and HCl (2-2) as demonstrated in preceding sections, it is possible to consider an O−H insertion reaction of formyl chloride (ClCHO) in water to produce chloromethanol diol [$CHCl(OH)_2$] (3-2) after the reaction (2-1). This alternative reaction pathway then proceeds by decomposition of $CHCl(OH)_2$ into formyl acid (HCOOH) and HCl in water (3-3) as shown in Figures 5 and 6c. Inspection of Figure 5 shows that reaction 3-2 proceeds mainly through a cyclic or cooperative mechanism with up to three H_2O molecules hydrating the carbonyl group. This is very similar to the water-catalyzed hydration reaction of HCHO with water (1-2) that we studied in a preceding subsection.

Examination of Table 1 and Figure 6c shows that the hydration reaction of ClCHO with water to form a chloromethanol diol $CHCl(OH)_2$ (3-2) possesses a much higher activation energy than those for the dissociation reaction of ClCHO into CO and HCl (2-2) with same number of water molecules in the reaction system. The barrier for the ClCHO + $n(H_2O) \rightarrow CHCl(OH)_2 + (n-1)H_2O$ where $n = 1$, 2, 3, 4 reaction remains

high (33.34 kcal/mol for one-water molecule, 29.58 kcal/mol for two-water molecules, and 30.48 kcal/mol for three-water molecules involved) since it is an O−H insertion reaction without an HX leaving group that can be solvated by water and is thus not significantly water-catalyzed by additional H_2O molecules beyond $n = 2$. The predicted larger 30.48 kcal/mol activation free energy for the three-water catalytic hydration reaction by 0.9 kcal/mol than the value for the two-water catalytic reaction indicates that the reaction has already reached a saturation limit. However, the subsequent decomposition of the $CHCl(OH)_2 + n(H_2O) \rightarrow HCOOH + HCl + n(H_2O)$ where $n = 0$, 1 reaction, which has an HCl leaving group, proceeds very easily (12.4 kcal/mol for one water molecule involved) like the other HCl elimination water-catalyzed reactions of halomethanols. The high barrier for the $ClCHO + nH_2O \rightarrow CHCl(OH)_2 + (n - 1)\ H_2O$ (where $n = 1$, 2, 3, 4) O−H insertion reaction (>29 kcal/mol) as compared to the low barrier for the $ClCHO + nH_2O \rightarrow CO + HCl + nH_2O$ (where $n = 1$, 2, 3, 4) HCl elimination reaction (about 18 kcal/mol) at the MP2/6-31+G** level of theory indicates that the major products are CO and HCl and the minor products are HCOOH and HCl for the reaction of $CHCl_2(OH)$ with water. This is consistent with the recent experimental observations that in aqueous solutions the generated ClCHO by decomposition of $CHCl_2$-(OH) was found to decompose into CO and HCl and traces of formic acid, HCOOH, and HCl.[19] The present theoretical study is also consistent with our recent combination of photochemistry experiments and theoretical calculations that found ultraviolet excitation of $CHBr_3$ in water gave almost complete conversion into three HBr leaving groups and CO (major product) and HCOOH (minor product) molecules.[45,46]

D. Proposed Simple Model to Explain the Water Catalysis of the Reactions of 1-1, 2-1, and 2-2 and Comparison with Available Experimental Kinetic Parameters. To mimic a real aqueous environment for the reactions, it is necessary to take the concentration of the $(RC)_{ijn}$ into account. Therefore, a kinetic treatment was done on the protocols of reactions 1-1, 2-1, and 2-2 to estimate the relevance of different reaction pathways and their contributions to each protocol. These results were then compared to the corresponding experimental observations in aqueous solution.[19] We assumed that H_2O, $CH_2Cl(OH)$, $CHCl_2$-(OH), ClCHO, and $(RC)_{ijn}$ are in equilibrium in an aqueous solution. On the basis of such an assumption, the contribution of each pathway to the overall pseudo-first-order rate constant for the decomposition of chloromethanol, dichloromethanol, and formyl chloride in aqueous solution will then depend on the equilibrium constant for the formation of $(RC)_{ijn}$ and the activation free energy of each channel with a different number of water molecules. Our proposed model is quite similar to that proposed by Eigen and Wolfe[42] for understanding the hydration mechanism of HCHO with water to produce methanediol.

The relationships between the analytical concentration of water (C_w)/solute (C_f) and the concentrations of each reactant species taken into account can be expressed in eqs 1 and 2:

$$C_w = [w] + [RC1] + 2[RC2] + 3[RC3] + 4[RC4] + 5[RC5] + 6[RC6] \quad (1)$$

$$C_f = [f] + [RCl] + [RC2] + [RC3] + [RC4] + [RC5] + [RC6] \quad (2)$$

Since

$$[RC1] = K_1[w][f];\ [RC2] = K_2[w]^2[f];\ [RC3] = K_3[w]^3[f];\ [RC4] = K_4[w]^4[f];\ [RC5] = K_5[w]^5[f];\ \text{and}\ [RC6] = K_6[w]^6[f] \quad (3)$$

The C_w and C_f can be written with regard to the concentration of water and solute monomers:

$$C_w = [w] + K_1[w][f] + 2K_2[w]^2[f] + 3K_3[w]^3[f] + 4K_4[w]^4[f] + 5K_5[w]^5[f] + 6K_6[w]^6[f]$$

$$C_f = [f] + K_1[w][f] + K_2[w]^2[f] + K_3[w]^3[f] + K_4[w]^4[f] + K_5[w]^5[f] + K_6[w]^6[f] \quad (4)$$

The values of [w] and [f] can be readily solved from the given value of C_w and C_f.

The overall reaction rate υ can be obtained from the sum of the partial reaction rates for all of the pathways:

$$\begin{aligned}\upsilon &= \upsilon 1 + \upsilon 2 + \upsilon 3 + \upsilon 4 + \upsilon 5 + \upsilon 6 + \upsilon 7 \\ &= k_0[f] + k_1[RC1] + k_2[RC2] + k_3[RC3] + k_4[RC4] + k_5[RC5] + k_6[RC6] \\ &= k_0[f] + k_1'[w][f] + k_2'[w]^2[f] + k_3'[w]^3[f] + k_4'[w]^4[f] + k_5'[w]^5[f] + k_6'[w]^6[f] \\ &= (k_0 + k_1'[w] + k_2'[w]^2 + k_3'[w]^3 + k_4'[w]^4 + k_5'[w]^5 + k_6'[w]^6)[f] \quad (5)\end{aligned}$$

where $k_n' = k_nK_n$ ($n = 1$, 2, 3, 4, 5, 6).

Substitution of eq 4 into eq 5 results in the pseudo-first-order reaction rate

$$\upsilon = kC_f \quad (6)$$

where

$$k = \frac{k_0 + k_1'[w] + k_2'[w]^2 + k_3'[w]^3 + k_4'[w]^4 + k_5'[w]^5 + k_6'[w]^6}{1 + K_1[w] + + K_2[w]^2 + K_3[w]^3 + K_4[w]^4 + K_5[w]^5 + K_6[w]^6}$$

The effective activation free energy, $\Delta G^{\ddagger}$, can be found from the Eyring eq 7

$$k = \frac{k_B T}{h} e^{-\Delta G^{\ddagger}/RT} \quad (7)$$

where k_B is the Boltzmann's constant and h is Planck's constant.

Table 3 collected the MP2/aug-cc-pVDZ single-point calculations at the MP2/6-31+G** optimized geometries for the activation free energies $\Delta G^{\ddagger}_{gas}$, rate constant k_{gas} for each reaction channels, stabilization free energies of RC $\Delta G_{RC}{}^{N}$ without BSSE corrections, $\Delta G_{RC}{}^{B}$ with BSSE corrections, and $\Delta G_{RC}{}^{G3MP2}$ from G3MP2 calculations[47] relative to separated reactants in gas phase and the activation free energies $\Delta G^{\ddagger}_{solv}$ (see computational details) and rate constant k_{solv} for each reaction channels in aqueous solutions for reactions 1-1, 2-1, and 2-2.

The gas phase stabilization free energies for the reactant clusters were carried out at the levels of MP2/aug-cc-pVDZ and G3MP2 theory[47] by the difference between the free energies of

RC and the separated reactants S + nH$_2$O, where S represents the substrates CH$_2$Cl(OH), CHCl$_2$(OH), and ClCHO. Examination of Table 3 shows that the calculated stabilization free energies (first column in Table 3) for RCs at the MP2/aug-cc-pVDZ level without BSSE corrections are quite similar to those obtained by higher level G3MP2 calculations for all of the (RC)$_{111-6}$, (RC)$_{211-6}$, and (RC)$_{221-4}$. This is somewhat surprising. We note that both G3[47] (3.33 and 1.98 kcal/mol for 373 and 298 K) and G3MP2[47] (3.64 and 2.24 kcal/mol for 373 and 298 K) calculations reproduced very well the experimental free energy[48] (3.34 and 1.95 kcal/mol at 373 and 298 K) for formation of water dimer from water molecules. Hence, we decide to obtain the stabilization free energies in gas phase and aqueous solution for the reactant clusters of (RC)$_{111-6}$, (RC)$_{211-6}$, and (RC)$_{221-4}$ by using either MP2/aug-cc-pVDZ or G3MP2 calculations as shown in Table 3. We noted that the stabilization energies from separated reactants to RC could be overestimated due to the effect of basis set superpostion error (BSSE). It is often necessary to make such a correction, and the counterpoise (CP) method is widely used for this purpose. However, a study on hydrogen-bonded dimers found the estimates of the effects of the BSSE by the CP method may not lead to better results since they do not provide quantitative information about the basis set deficiencies.[49] Therefore, the stabilization free energies with BSSE corrections could be regarded as an upper bound estimate of stabilities for RCs. We believe that our current stabilization free energies from the calculations at the MP2/aug-cc-pVDZ level of theory without BSSE corrections or from the G3MP2 level of theory probably provide a good estimate for the stabilities of the RCs in the gas and solution phases. These results were then used to do further kinetic analysis calculations for comparison with experimental kinetic data.

It is interesting to compare the activation free energies in the gas phase and in aqueous solution vs the number of water molecules. Inspection of Table 3 and Figure 9 shows that the reaction barriers for the solvated reactions with small water clusters are reduced by 0−7 kcal/mol as compared to those of the gas phase for $n \leq 4$. However, the gas and aqueous solution results for the barriers become closer after $n = 4$. It is evident that for reactions 1-1, 2-1, and 2-2, both the gas and the solution phase results predict very similar activation free energies for $n = 4$. The MP2/aug-cc-pVDZ-DPCM-BONDI model gives very close activation energies for reaction 2-2 as compared to the MP2/aug-cc-PVDZ + B3LYP/aug-cc-pVDZ-DPCM-BONDI model results as shown in Figure 9. However, for reactions 1-1 and 2-1, the solvation model has a small inhibitory effect for $n > 4$, in which slightly larger activation free energies were obtained as compared to those of gas phase. This implies that it is necessary to build up a solvated reactant water cluster by explicitly adding water molecules one by one. Note that at least four water molecules or $n \geq 4$ were needed to build up the active species that probably makes the predominant contribution to the overall reactions in aqueous solutions.

Table 4 summarizes the results of the kinetics model analysis, using $C_w = 55$ M and $C_f = 1$ M. In the gas phase model, the activation free energies $\Delta G^{\ddagger}_{gas}$ and stabilization free energies $\Delta G_{RC}{}^{N}$, $\Delta G_{RC}{}^{B}$, and $\Delta G_{RC}{}^{G3MP2}$ of different RCs in Table 3 were used to compute and mimic the kinetics data in a real aqueous environment. In the D-PCM model treatment, the activation free energies $\Delta G^{\ddagger}_{solv}$ in Table 3 and stabilization free energies from G3MP2[45] in Table 3 were used to compute and mimic the kinetics data in a real aqueous environment. Figure 9 plotted the reaction barriers vs the number of water molecules (n) at the MP2/aug-cc-pVDZ level of theory in the gas phase and in an aqueous solution. In reaction 2-2, both the B3LYP-DPCM and the MP2-DPCM models were used to calculate the solvation energies for the RCs and TSs.

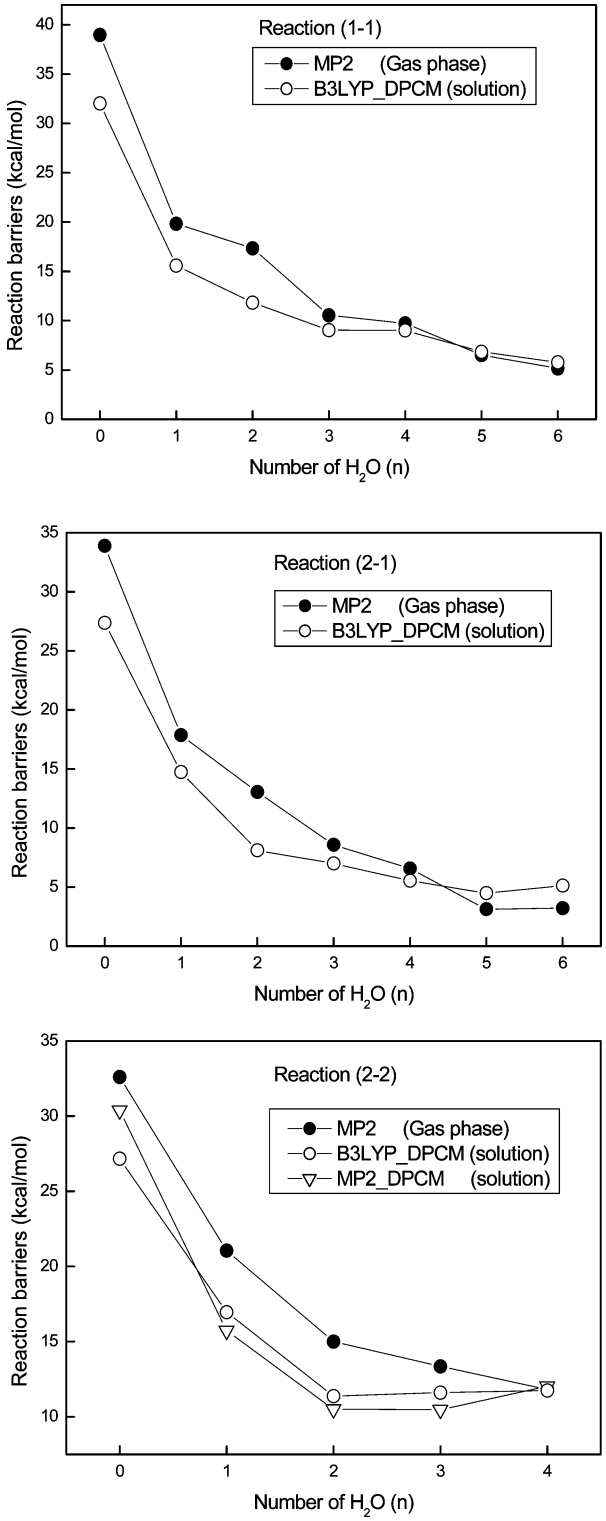

Figure 9. Plots of the gas phase and aqueous solution activation free energies at the MP2/aug-cc-pVDZ level vs the number of water molecules for reactions (a) (1-1) CH$_2$(OH)Cl + nH$_2$O → HCHO + nH$_2$O + HCl; (b) (2-1) CH(OH)Cl$_2$ + nH$_2$O → ClCHO + nH$_2$O + HCl; and (c) (2-2) ClCHO + nH$_2$O → CO + HCl + nH$_2$O.

Inspection of Table 4 shows that in the gas phase kinetic treatment, the effective activation free energies for reaction 2-2 were predicted to be 11.86 kcal/mol from $\Delta G^{\ddagger}_{gas}$ and $\Delta G_{RC}{}^{N}$ and $\Delta G_{RC}{}^{G3MP2}$. The overall pseudo-first-order reaction rates were predicted to be 1.2×10^4 s^{-1}. With the activation free

TABLE 4: Concentrations of H_2O and $(RC)_{ijn}$ and Contributions of the Different Channels, Pseudo-First-Order Rate Constants (k, s^{-1}), and Effective Activation Free Energies ($\Delta G^{\ddagger}$, kcal mol^{-1}) Are Collected in This Table[a]

	gas phase cluster model						D-PCM model	
	no BSSE		BSSE		G3MP2		G3MP2	
	concn (M)	contrib.	concn (M)	contrib.	concn (M)	contrib.	concn (M)	contrib.
	1-1: $CH_2(OH)Cl + nH_2O \rightarrow HCHO + nH_2O + HCl$ ($n = 0, 1, 2, ..., 6$)							
H_2O	50.43		53.35		50.84		50.84	
$(RC)_{110}$	2.09×10^{-5}	0.0000	2.01×10^{-1}	0.0000	1.64×10^{-5}	0.0000	1.64×10^{-5}	0.0000
$(RC)_{111}$	2.35×10^{-4}	0.0000	2.03×10^{-1}	0.0000	1.49×10^{-4}	0.0000	1.49×10^{-4}	0.0000
$(RC)_{112}$	4.61×10^{-3}	0.0000	4.34×10^{-1}	0.0000	1.49×10^{-3}	0.0000	1.49×10^{-3}	0.0000
$(RC)_{113}$	4.34×10^{-2}	0.0000	7.76×10^{-2}	0.0234	1.80×10^{-2}	0.0000	1.80×10^{-2}	0.0010
$(RC)_{114}$	4.00×10^{-1}	0.0015	8.16×10^{-2}	0.0986	8.60×10^{-1}	0.0060	8.60×10^{-1}	0.0501
$(RC)_{115}$	4.85×10^{-1}	0.4192	3.14×10^{-3}	0.8538	6.29×10^{-2}	0.0981	6.29×10^{-2}	0.1433
$(RC)_{116}$	6.69×10^{-2}	0.5792	8.91×10^{-6}	0.0242	5.73×10^{-2}	0.8959	5.73×10^{-2}	0.8056
k_{calcd}	1.19×10^{8}		3.78×10^{5}		6.58×10^{7}		2.63×10^{7}	
$\Delta G^{\ddagger}$	6.43		9.84		6.78		7.33	
k_{exp}							NA	
	2-1: $CH(OH)Cl_2 + nH_2O \rightarrow ClCHO + nH_2O + HCl$ ($n = 0, 1, 2, ..., 6$)							
H_2O	51.12		53.88		51.18		51.18	
$(RC)_{210}$	1.69×10^{-4}	0.0000	1.59×10^{-1}	0.0000	4.02×10^{-5}	0.0000	4.02×10^{-5}	0.0000
$(RC)_{211}$	1.03×10^{-2}	0.0000	6.35×10^{-1}	0.0000	1.32×10^{-3}	0.0000	1.32×10^{-3}	0.0000
$(RC)_{212}$	5.22×10^{-2}	0.0000	1.29×10^{-1}	0.0002	1.50×10^{-2}	0.0000	1.50×10^{-2}	0.0002
$(RC)_{213}$	4.07×10^{-1}	0.0002	7.60×10^{-2}	0.1997	2.27×10^{-1}	0.0004	2.27×10^{-1}	0.0208
$(RC)_{214}$	2.46×10^{-1}	0.0028	7.34×10^{-4}	0.0584	7.03×10^{-1}	0.0413	7.03×10^{-1}	0.7691
$(RC)_{215}$	1.53×10^{-1}	0.5718	2.78×10^{-5}	0.7312	2.20×10^{-2}	0.4286	2.20×10^{-2}	0.1411
$(RC)_{216}$	1.32×10^{-1}	0.4253	4.66×10^{-7}	0.0105	3.17×10^{-2}	0.5297	3.17×10^{-2}	0.0688
k_{calcd}	8.42×10^{9}		1.20×10^{6}		1.62×10^{9}		4.93×10^{8}	
$\Delta G^{\ddagger}$	3.91		9.15		4.88		5.59	
k_{exp} [19]							$>4.0 \times 10^{4}$	
	2-2: $ClCHO + nH_2O \rightarrow CO + HCl + nH_2O$ ($n = 0, 1, 2, ..., 4$)							
H_2O	51.18		54.90		51.15		51.15	
$(RC)_{220}$	2.75×10^{-2}	0.0000	9.18×10^{-1}	0.0000	1.54×10^{-2}	0.0000	1.54×10^{-2}	0.0000
$(RC)_{221}$	9.81×10^{-3}	0.0000	7.32×10^{-2}	0.0000	3.28×10^{-3}	0.0000	3.28×10^{-3}	0.0000
$(RC)_{222}$	9.55×10^{-3}	0.0000	4.89×10^{-3}	0.0095	8.39×10^{-3}	0.0000	8.39×10^{-3}	0.0156
$(RC)_{223}$	2.36×10^{-2}	0.0019	1.27×10^{-3}	0.0408	5.83×10^{-2}	0.0047	5.83×10^{-2}	0.0747
$(RC)_{224}$	9.30×10^{-1}	0.9981	2.20×10^{-3}	0.9497	9.15×10^{-1}	0.9952	9.15×10^{-1}	0.9097
k_{calcd}	1.25×10^{4}		3.10×10^{1}		1.23×10^{4}		1.48×10^{4}	
$\Delta G^{\ddagger}$	11.86		15.41		11.86		11.75	
k_{exp} [19]							1.0×10^{4}	

[a] The values of rate constants from experiments (k_{exp}) are also shown here for comparison.

energies $\Delta G^{\ddagger}_{solv}$ obtained from the MP2/aug-cc-PVDZ + B3LYP/aug-cc-pVDZ-DPCM-BONDI calculations in aqueous solutions and the stabilization free energies from G3MP2 calculations, the rate constant was predicted to be 1.5×10^4 s^{-1}. These results are all in excellent agreement with the experimental rate constant of 10^4 s^{-1}.[19] The largest contribution to the overall reaction comes from $(RC)_{224}$ to $(TS)_{224}$. The concentration of the active species is also the largest among the five species $(RC)_{220-5}$ including ClCHO or $(RC)_{220}$. However, using the stabilization free energies $\Delta G_{RC}{}^{B}$ with a BSSE correction, the rate constant was predicted to be 3×10^1 s^{-1} and this underestimates the experimental results[19] too much.

As shown in Table 4, the effective activation free energies for reaction 2-1 were predicted to be 3.91 and 4.88 kcal/mol, respectively, with $\Delta G^{\ddagger}_{gas}$ and $\Delta G_{RC}{}^{N}$ and $\Delta G_{RC}{}^{G3MP2}$ for the gas phase model treatment. The overall pseudo-first-order reaction rates for this reaction were predicted to be 8.4×10^9 and 1.6×10^9 s^{-1}. The D-PCM model predicted an activation energy of 5.59 kcal/mol and a rate constant of 4.9×10^8 s^{-1}. Considering the lower bound of the experimentally estimated rate constant of 4.0×10^4 s^{-1}, the agreement between experiment and theory is reasonable. The main contribution to this pseudo first-order reaction comes from $(RC)_{214-6}$ depending on the stabilization free energies of RCs predicted at different levels of theory. The biggest contribution to the overall reaction comes from $(RC)_{214}$ in aqueous solutions, which is predicted to have the largest concentration as compared to the other active species. It is interesting to note that our results are reasonably consistent with a very recent study,[51] in which the water tetramer was predicted to have the most negative ΔG^0 (−1.66 kcal/mol, 298 K) for tetramerization of water from monomer at the G3 level. This may be consistent with the water tetramer-based reactive species RC_{224} or RC_{214} being the main contributor to the decomposition reaction in aqueous solutions. ΔG^0 values for the cyclic water pentamer, the cyclic hexamer, the cagelike water hexamer, and the prismlike hexamer were predicted to be −0.46, 1.77, 3.66, and 4.07 kcal/mol, respectively, at the G3 level of theory.[51] These stabilization free energies for formation of water clusters are comparable with our predicted free energies of the active RCs in Table 3. Therefore, the active species with four, five, and six water molecules may be expected to mainly contribute to the decomposition reaction of chloromethanols and formyl chloride in aqueous solutions.[51]

Reaction 1-1 was predicted to be slightly slower than reaction 2-1. The rate constant was predicted in the range of 3.8×10^5 to $\sim 1.2 \times 10^8$ s^{-1}. Although there are no aqueous experimental kinetics data for reaction 1-1, the predicted smaller rate constant for 1-1 than reaction 2-1 in aqueous solution is consistent with the fact that in the gas phase, the decomposition reaction of 1-1 is slower than 2-1.

In summary, both gas phase cluster and polarized continuum D-PCM models can reasonably model these decomposition reactions of chloromethanols and formyl chloride in aqueous solutions by considering at least four explicitly solvated water

molecules in the reactant clusters. This suggests that the first 4−6 explicitly coordinated water molecules in the solvation shell of the reacting system make the predominant solvent contribution to these water-assisted reactions. This is consistent with the water-catalyzed nature of these reactions in which the water solvent molecules act to couple the proton transfer from the reactant molecule to the solvation of the Cl^- leaving group in the HCl elimination reactions. These water molecules directly participate in the main reaction coordinate and thus have the largest effect on the reaction pathway and the energy of activation. Additional water solvent molecules further away will have much smaller effects on the reaction pathway and energy of activation because they do not directly participate in coupling the proton transfer from the reactant molecule to the solvation of the Cl^- leaving group in the HCl elimination reactions.

E. Discussion of the Water-Catalyzed HCl Elimination Reactions and Likely Implications for Decomposition of Halomethanols and Haloformaldehyes in Aqueous Environments. Our results here indicate that water molecules greatly assist in the decomposition of chlorinated methanols and formyl chloride with the rate of decomposition becoming greater by 7 or 8 orders of magnitude in aqueous solution as compared to the gas phase reaction with one water molecule. This is consistent with experimental results in the literature that show a similar 7−8 order magnitude enhancement of the rate of decomposition of these chlorinated methanols and formyl chloride in aqueous solution as compared to their gas phase decomposition. Calculations that explicitly coordinate water molecules and also consider the bulk effect of the water solution on the reaction system were able to predict a rate constant for the decomposition of formyl chloride in aqueous solution that was in excellent agreement with the experimentally measured value in the literature. For example, the activation free energies $\Delta G^{\ddagger}_{solv}$ obtained from MP2/aug-cc-pVDZ + B3LYP/aug-cc-pVDZ-DPCM-BONDI calculations in aqueous solutions and the stabilization free energies from G3MP2 calculations were used to predict a rate constant of $1.5 \times 10^4\ s^{-1}$, which is in excellent agreement with the experimental rate constant of $10^4\ s^{-1}$.[19]

Our results indicate that water molecules greatly catalyze (or assist) the HCl elimination reactions of chlorinated methanols and formyl chloride. This water catalysis appears to occur by a simultaneous proton transfer of the H atom from the molecular species to the O atom of a water molecule and solvation of the leaving Cl atom of the molecular species by H···Cl interactions with the water solvent molecules. Thus, the water solvent molecules enable the HX elimination reaction to be coupled to the dissociation of molecular HCl into H^+ and Cl^- ions [or H_3O^+ and $Cl^-(H_2O)_n$ ions], which is exothermic and occurs easily in the presence of water. This coupling of the HCl dissociation into its ions in aqueous solution with the HCl elimination reaction helps drive the reaction. This allows cleavage of the O−H and C−Cl bonds in chlorinated methanols and the C−H and C−Cl bonds in formyl chloride to occur with low barriers to reaction in water-solvated environments. Because C−Br and C−I bonds are weaker than a C−Cl bond and the HX (X═Cl, Br, I) dissociation processes in aqueous solution are similar to one another, we think that this type of water catalysis will be a general phenomena for the HX elimination reactions of halogenated methanols and halogenated formaldehydes in aqueous environments. We expect that this type of water catalysis will also occur in HX elimination reactions for other molecules, but this remains to be explored in the future.

Our present work also has some interesting implications for the mechanism of the oxidative decay cascade that can be observed by conductance changes in advanced oxidation processes. These advanced oxidation processes such as UV/hydrogen peroxide, UV/ozone, ozone/hydrogen peroxide, and electron beam radiation are used to induce decomposition of chlorinated hydrocarbons in drinking water supplies, and chlorinated methanols and formyl chloride have been observed as chemical intermediates in some of these degradation reactions.[19] The work here in conjunction with the previous report indicates that water takes on a rather active participation in the dehalogenation of the chlorinated methanol and formyl chloride intermediates and acts to drive the dehalogenation process. This has important implications for the design of energy efficient, robust, and environmentally friendly catalysts for degradation of chlorinated and other halogenated hydrocarbon pollutants in drinking water supplies. Conceivably, water molecules can be employed by a suitably designed catalyst to help drive the reactions and the ionic products used to regenerate the catalysts. One could also use the HX leaving group from the water-catalyzed decomposition of halogenated methanols or formaldehydes to promote acid-catalyzed pathways in the design of a practical catalyst for the degradation of halogenated hydrocarbons.

Our present results also have some interesting implications for the decomposition of halogenated hydrocarbons in the natural environment. In the presence of one or more water molecules, the chlorinated methanols and formyl chloride examined here decompose much more easily than isolated molecules. A recent experimental study observed that the water dimer is present at 294 K and speculated that larger water clusters with $n = 3-6$ may also exist in quantities comparable to ambient aerosol in the background troposphere.[50] A very recent theoretical study used CBS-APNO free energies to estimate the number of higher order water clusters that found excellent agreement between a computed concentration of 4×10^{14} water dimers/cm^3 as compared to an experimental measurement of 6×10^{14} water dimers/cm^3 at a temperature of 292.4 K.[50,51] Further theoretical work estimated that the concentrations of water trimers, tetramers, pentamers, and hexamers at 298.15 K produced from individual water molecules were 2.6×10^{12}, 5×10^{11}, 2.5×10^{10}, and 3×10^4 clusters/cm^3.[51] The estimated concentrations of the trimer and tetramer water clusters are only 2−3 orders of magnitude smaller than that of the water dimers at ambient temperatures in the lower troposphere. Our present results for the water-catalyzed decomposition of chloromethanol and dichloromethanol found that the rate of decomposition changed by about 4−5 orders of magnitude upon going from reaction with two water molecules to three or four water molecules. This combined with the recent estimates of the concentrations of water dimers and higher oligomers suggests that decomposition of chlorinated methanols (and likely other halogenated methanols) via the larger water clusters such as trimers, tetramers, and hexamers could be comparable or even larger than found for water dimers. Our present results in conjunction with the recent estimates of the concentrations of water clusters suggest that decomposition chlorinated methanols (and likely other halogenated methanols) may occur predominantly via reaction with water and water clusters in the atmosphere rather than via isolated molecule decomposition reactions. Similarly, our present results for the water-catalyzed decomposition of chloromethanol and dichloromethanol found that the rate of decomposition changed by about 4−7 orders of magnitude upon going from reaction with one water molecules to reaction with three or four water molecules. This also suggests decomposition of formyl chloride (and likely other formyl halides) via the larger

oligomers such as trimers, tetramers, and hexamers could be comparable or even larger than found for water dimers. Our results for formyl chloride also suggest that decomposition of formyl chloride (and likely other formyl halides) may occur mostly via reaction with water and water clusters in the atmosphere rather than via isolated molecule decomposition reactions. Our results also indicate that the decomposition of chlorinated methanols and formyl chloride (and likely other halogenated methanols and formaldehydes) will undergo very efficient decomposition at surfaces, in interfacial regions, and in bulk water environments such as ice and water particles in the natural environment.

We note that it has been suggested that water clusters could significantly assist certain reactions to occur in the atmosphere such as in the oxidation of SO_3 to H_2SO_4 and other reactions.[50−55] The water-assisted mechanism that we have presented here for the HCl elimination reactions of chlorinated methanols and formyl chloride may occur for many other similar reactions where the water molecules can assist or catalyze a molecular leaving group into ions. At this point, it is not clear how general these types of water-assisted reactions are in chemistry. It is also not clear what the actual effect of these kinds of reactions have for a number of species relevant to atmospheric chemistry and the natural environment. We anticipate that this will be a growing area of research to which many different experimental and theoretical approaches may be applied by a number of different research groups.

IV. Summary and Concluding Remarks

An ab initio investigation of the reactions of chloromethanol, dichloromethanol, and formyl chloride with water was presented in which water molecules (up to six) were explicitly included in the reaction system. The decomposition reactions of the chlorinated methanols and formyl chloride were found to be significantly catalyzed by water molecules with the decomposition becoming faster as the number of water molecules increases. Predicted rate constants for the decomposition of formyl chloride (from 1.2×10^4 to 1.5×10^4 s^{-1}) were in good agreement with the experimental value of 1×10^4 s^{-1} measured in aqueous solution. Both gas phase cluster and polarized continuum D-PCM models are able to reasonably simulate these decomposition reactions of chloromethanols and formyl chloride in aqueous solutions by considering at least four explicitly solvated water molecules in the reactant clusters. This indicates that the first 4−6 water molecules explicitly included in the solvation shell of the reacting system make the predominant solvent contribution to these water-catalyzed reactions. This is consistent with the water-catalyzed character of these reactions where the water molecules couple the proton transfer from the reactant molecule to the solvation of the Cl^- leaving group in the HCl elimination reactions and thus have the largest effect on the reaction pathway and the energy of activation. We briefly discuss our results in relation to several recent experimental and theoretical studies on water clusters and possible implications for the decomposition of halogenated methanols and formyl chlorides in aqueous solution and in the natural environment.

Acknowledgment. This research was supported by grants from the Research Grants Council of Hong Kong (HKU/7036/04P) to D.L.P.

Supporting Information Available: Cartesian coordinates, total energies (a.u.), vibrational zero-point energies (a.u.), enthalpies (a.u.), and free energies (a.u.) for the stationary structure. This material is available free of charge via the Internet at http://pubs.acs.org.

References and Notes

(1) Wayne, R. P. *Chemistry of Atmospheres*, 3rd ed.; Oxford University Press: Oxford, United Kingdom, 2000.

(2) Grotheer, H. H.; Riekert, G.; Meier, U.; Just, Th. Symp. (Int.) Gas Kinet. [Proc.] Bordeaux, France, 1986.

(3) Jenkin, M. E.; Cox, R. A.; Hayman, G. D.; Whyte, L. J. *J. Chem. Soc., Faraday Trans. 2* **1988**, *84*, 913.

(4) Knuttu, H.; Dahlqvist, M.; Murto, J.; Räsänen, M. *J. Phys. Chem.* **1988**, *92*, 1495−1502.

(5) Tyndall, G. S.; Wallington, T. J.; Hurley, M. D.; Schneider, W. F. *J. Phys. Chem.* **1993**, *97*, 1576−1582.

(6) Wallington, T. J.; Schneider, W. F.; Barnes, I.; Becker, K. H.; Sehested, J.; Nielsen, O. J. *Chem. Phys. Lett.* **2000**, *322*, 97−102.

(7) Scheytt, H.; Esrom, H.; Prager, L.; Mehnert, R.; von Sontag, C. In *Nonthermal Plasma Techniques for Pollution Control, Part B*; Penetrante, B. M., Schultheis, S. E., Eds.; Springer-Verlag: Heidelberg 1993; pp 91−101.

(8) Mertens, R.; von Sontag, C. *Angew. Chem., Int. Ed. Engl.* **1994**, *33*, 1262−1264.

(9) Mertens, R.; von Sontag, C. *J. Chem. Soc., Perkins Trans. 2* **1994**, 2181−2185.

(10) Mertens, R.; von Sontag, C. *Angew. Chem., Int. Ed. Engl.* **1994**, *33*, 1259−1261.

(11) Dowideit, P.; von Sontag, C.; Leitzke, O. *GWF, Wasser-Abwasser* **1996**, *137*, 268.

(12) Von Sontag, C.; Mark, G.; Mertens, R.; Schuchmann, M. N.; Schuchmann, H.-P. *J. Water Supply Res. Technol.-Aqua* **1993**, *42*, 201−211.

(13) Buxton, G. V.; Greenstock, C.-L.; Helman, W. P.; Ross, A. B. *J. Phys. Chem. Ref. Data* **1988**, *17*, 513−886.

(14) Neta, P.; Huie, R. E.; Ross, A. B. *J. Phys. Chem. Ref. Data* **1988**, *17*, 1027−1284.

(15) Asmus, K.-D. *Int. J. Radiat. Phys. Chem.* **1972**, *4*, 417−437.

(16) Asmus, K.-D. *Methods Enzymol.* **1984**, *105*, 167−178.

(17) Von Sontag, C.; Schuchmann, H.-P. *Methods Enzymol.* **1994**, *233*, 3−20.

(18) Bothe, E.; Janata, E. *Radiat. Phys. Chem.* **1994**, *44*, 455−458.

(19) Dowidiet, P.; Mertens, R.; von Sontag, C. *J. Am. Chem. Soc.* **1996**, *118*, 11288−11292.

(20) Hisatsune, C.; Heicklen, J. *Can. J. Spectrosc.* **1973**, *18*, 77−81.

(21) Libuda, H. G.; Zabel, F.; Fink, E. H.; Becker, K. H. *J. Phys. Chem.* **1990**, *94*, 5860−5865.

(22) Tyrrell, J.; Lewis-Bevan, W. *J. Phys. Chem.* **1992**, *96*, 1691−1696.

(23) Francisco, J. S.; Williams, I. H. *J. Am. Chem. Soc.* **1993**, *115*, 3746−3751.

(24) Butler, R.; Snelson, A. J. *Air Pollut. Control Assoc.* **1979**, *29*, 833.

(25) Gonzalez, C.; Schlegel, H. B. *J. Chem. Phys.* **1989**, *90*, 2154−2161. (b) Gonzalez, C.; Schlegel, H. B. *J. Phys. Chem.* **1990**, *94*, 5523−5527.

(26) Miertus, S.; Scrocco, E.; Tomasi, J. *Chem. Phys.* **1981**, *55*, 117. (b) Miertus, S.; Tomasi, J. *Chem. Phys.* **1982**, *65*, 239. (c) Cossi, M.; Barone, V.; Cammi, R.; Tomasi, J. *Chem. Phys. Lett.* **1996**, *255*, 327. (d) Cossi, M.; Scalmani, G.; Rega, N.; Barone, V.; Cammi, R. *J. Chem. Phys.* **2002**, *117*, 43.

(27) Bondi A. *J. Phys. Chem.* **1964**, *68*, 441.

(28) Fu, Y.; Liu, L.; Li, R.-Q.; Liu, R.; Guo, Q.-X. *J. Am. Chem. Soc.* **2004**, *126*, 814.

(29) Frisch, M. J.; Trucks, G. W.; Schlegel, H. B.; Scuseria, G. E.; Robb, M. A.; Cheeseman, J. R.; Zakrzewski, V. G.; Montgomery, J. A., Jr.; Stratmann, R. E.; Burant, J. C.; Dapprich, S.; Millam, J. M.; Daniels, A. D.; Kudin, K. N.; Strain, M. C.; Farkas, O.; Tomasi, J.; Barone, V.; Cossi, M.; Cammi, R.; Mennucci, B.; Pomelli, C.; Adamo, C.; Clifford, S.; Ochterski, J.; Petersson, G. A.; Ayala, P. Y.; Cui, Q.; Morokuma, K.; Malick, D. K.; Rabuck, A. D.; Raghavachari, K.; Foresman, J. B.; Cioslowski, J.; Ortiz, J. V.; Baboul, A. G.; Stefanov, B. B.; Liu, G.; Liashenko, A.; Piskorz, P.; Komaromi, I.; Gomperts, R.; Martin, R. L.; Fox, D. J.; Keith, T.; Al-Laham, M. A.; Peng, C. Y.; Nanayakkara, A.; Gonzalez, C.; Challacombe, M.; Gill, P. M. W.; Johnson, B.; Chen, W.; Wong, M. W.; Andres, J. L.; Gonzalez, C.; Head-Gordon, M.; Replogle, E. S.; Pople, J. A. *Gaussian 98 revision A.7 and Gaussian 03 revision B.05*; Gaussian Inc.: Pittsburgh, PA, 1998, 2003.

(30) Gruenloh, C. J.; Carney, J. R.; Arrington, C. A.; Zwier, T. S.; Fredericks, S. Y.; Jordan, K. D. *Science* **1997**, *276*, 1678. (b) Gruenloh, C. J.; Carney, J. R.; Hagemeister, F. C.; Arrington, C. A.; Zwier, T. S. *J. Chem. Phys.* **1998**, *109*, 6601. (c) Gruenloh, C. J.; Zwier, T. S.; Wood, J. T., III; Jordan, K. D. *J. Chem. Phys.* **2000**, *113*, 2290.

(31) Buck, U.; Ettischer, I.; Melzer, M.; Buch, V.; Sadlej, J. *Phys. Rev. Lett.* **1998**, *80*, 2578. (b) Brudermann J.; Melzer, M.; Buck, U.; Kazimirski;

J. K.; Sadlej, J.; Buch, V. *J. Chem., Phys.* **1999**, *110*, 10649. (c) Sadlej, J.; Buch, V.; Kazimirski, J. K.; Buck, U. *J. Phys. Chem. A* **1999**, *103*, 4933.

(32) Kim, K. S.; Dupuis, M.; Lie, G. C.; Clementi, E. *Chem. Phys. Lett*. **1986**, *131*, 451. (b) Kim, J.; Mhin, B. J.; Lee S. J.; Kim, K. S. *Chem. Phys. Lett*. **1994**, *219*, 243. (c) Kim, J.; Majumdar, D.; Lee, H. M.; Kim, K. S. *J. Chem. Phys.* **1999**, *110*, 9128. (d) Kim, K. S.; Tarakeshwar, P.; Lee, J. Y. *Chem. Rev.* **2000**, *100*, 4145.

(33) Lee, H. M.; Kim, K. S. *J. Chem. Phys.* **2002**, *117*, 706−708.

(34) Lee, H. M.; Suh, S. B.; Lee, J. Y.; Tarakeshwar, P.; Kim, K. S. *J. Chem. Phys.* **2000**, *112*, 9759. (b) Lee, H. M.; Suh, S. B.; Lee, J. Y.; Tarakeshwar, P.; Kim, K. S. *J. Chem. Phys.* **2001**, *114*, 3343.

(35) Cabaleiro-Lago, E. M.; Hermida-Ramon, J. M.; Rodriguez-Otero, J. *J. Chem. Phys.* **2002**, *117*, 3160−3168.

(36) Milet, A.; Struniewicz, C.; Moszynski, R.; Wormer, P. E. S. *J. Chem. Phys.* **2001**, *115*, 349−356.

(37) Amirand, C.; Maillard, D. *J. Mol. Struct.* **1988**, *176*, 181.

(38) Lee, C.; Sosa, C.; Planas, M.; Novoa, J. J. *J. Chem. Phys.* **1996**, *104*, 7081. (b) Planas, M.; Lee, C.; Novoa, J. J. *J. Phys. Chem.* **1996**, *100*, 16495. (c) Re, S.; Osamura, Y.; Suzuki, Y.; Schaefer, H. F. *J. Chem. Phys.* **1998**, *109*, 973. (d) Smith, A.; Vincent, M. A.; Hillier, I. H. *J. Phys. Chem. A* **1999**, *103*, 1132. (e) Bacelo, D. E.; Binning, R. C.; Ishikawa, Y. *J. Phys. Chem. A* **1999**, *103*, 4631.

(39) Le Botlan, D. J.; Mechin, B. G.; Martin, G. J. *Anal. Chem.* **1983**, *55*, 587−591.

(40) Bell, R. P. *Adv. Phys. Org. Chem.* **1966**, *4*, 1−29.

(41) Zavitsas, A. A.; Coffiner, M.; Wiseman, T.; Zavitsas, L. R. *J. Phys. Chem.* **1970**, *74*, 2746−2750.

(42) Wolfe, S.; Kim, C.-K.; Yang, K.; Weinberg, N.; Shi, Z. *J. Am. Chem. Soc.* **1995**, *117*, 4240−4260. (b) Eigen, M. *Discuss. Faraday Sac.* **1965**, *39*, 7−15. (c) Mó, O.; Yáñez, M.; Elguero, J. *J. Chem. Phys.* **1992**, *97*, 6628−6638. (d) Koehler, J. E. H.; Saenger, W.; Lesyng, B. *J. Comput. Chem.* **1987**, *8*, 1090−1098. (e) Corongiu, G.; Clementi, E. *Chem. Phys. Lett.* **1993**, *214*, 367−372. (f) Kim, J.; Mhin, B. J.; Lee, S. J.; Kim, K. S. *Chem. Phys. Lett.* **1994**, *219*, 243−246 and references therein.

(43) Kwok, W. M.; Zhao, C. Y.; Guan, X.; Li, Y.-L.; Du, Y.; Phillips, D. L. *J. Chem. Phys.* **2004**, *120*, 9017. (b) Guan, X.; Du, Y.; Li, Y. L.; Kwok, W. M.; Phillips, D. L. *J. Chem. Phys*. **2004**, *121*, 8399. (c) Lin, X.; Zhao, C.; Phillips, D. L. *Chem. Phys. Lett.* **2004**, *397*, 488. (d) Lin, X.; Guan, X.; Kwok, W. M.; Zhao, C.; Du, Y.; Li, Y. L.; Phillips, D. L. *J. Phys. Chem. A* **2005**, *109*, 981. (e) Du, Y.; Guan, X.; Kwok, W. M.; Chu, L. M.; Phillips, D. L. *J. Phys. Chem. A* **2005**, *109*, 5872.

(44) Francisco, J. S.; Zhao, Y. *J. Chem. Phys.* **1992**, *96*, 7587.

(45) Kwok, W. M.; Zhao, C. Y.; Li, Y.-L.; Guan, X.; Phillips, D. L. *J. Chem. Phys.* **2004**, *120*, 3323.

(46) Kwok, W. M.; Zhao, C. Y.; Li, Y.-L.; Guan, X.; Wang, D. Q.; Phillips, D. L. *J. Am. Chem. Soc.* **2004**, *126*, 3119. (b) Zhao, C.; Lin, X.; Kwok, W. M.; Guan, X.; Du, Y.; Wang, D.; Hung, K. F.; Phillips, D. L. *Chem. Eur. J.* **2005**, *11*, 1093.

(47) Curtiss, L. A.; Raghavachari, K.; Redfern, P.; Rassolov, C. V.; Pople, J. A. *J. Chem. Phys.* **1998**, *109*, 7764. (b) Curtiss, L. A.; Redfern, P. C.; Raghavachari, K.; Rassolov, V.; Pople, J. A. *J. Chem. Phys.* **1999**, *110*, 4703.

(48) Curtiss, L. A.; Frurip, L. A.; Blander, M. *J. Chem. Phys.* **1979**, *71*, 2703.

(49) Frisch, M. J.; Del Bene, J. E.; Binkley, J. S.; Schaefer, H. F., III. *J. Chem. Phys.* **1986**, *84*, 2279. (b) Halkier, A.; Klopper, W.; Helgaker, T.; Jørgensen, P.; Taylor, P. R. *J. Chem. Phys.* **1999**, *111*, 9157.

(50) Pfeilsticker, K.; Lotter, A.; Peters, C.; Bösch, H. *Science* **2003**, *300*, 2078.

(51) Dunn, M. E.; Pokon, E. K.; Shields, G. C. *J. Am. Chem. Soc*. **2004**, *126*, 2647.

(52) Loerting, T.; Liedl, K. R. *Proc. Natl. Acad. Sci. U.S.A.* **2000**, *97*, 8874.

(53) Jayne, J. T.; Pöschl, U.; Chen, Y.-M.; Dai, D.; Molina, L. T.; Worsnop, D. R.; Kolb, C. E.; Molina, M. J. *J. Phys. Chem. A* **1997**, *101*, 10000.

(54) Huneycutt, A. J.; Saykally, R. J. *Science* **2003**, *299*, 1329.

(55) Aloisio, S.; Francisco, J. S.; Friedl, R. R. *J. Phys. Chem. A* **2000**, *104*, 6597.